

Flavoprotein monooxygenases

Versatile biocatalysts

Paul, Caroline E.; Eggerichs, Daniel; Westphal, Adrie H.; Tischler, Dirk; van Berkel, Willem J.H.

DOI

[10.1016/j.biotechadv.2021.107712](https://doi.org/10.1016/j.biotechadv.2021.107712)

Publication date

2021

Document Version

Final published version

Published in

Biotechnology Advances

Citation (APA)

Paul, C. E., Eggerichs, D., Westphal, A. H., Tischler, D., & van Berkel, W. J. H. (2021). Flavoprotein monooxygenases: Versatile biocatalysts. *Biotechnology Advances*, 51, Article 107712. <https://doi.org/10.1016/j.biotechadv.2021.107712>

Important note

To cite this publication, please use the final published version (if applicable). Please check the document version above.

Copyright

Other than for strictly personal use, it is not permitted to download, forward or distribute the text or part of it, without the consent of the author(s) and/or copyright holder(s), unless the work is under an open content license such as Creative Commons.

Takedown policy

Please contact us and provide details if you believe this document breaches copyrights. We will remove access to the work immediately and investigate your claim.



Contents lists available at ScienceDirect

Biotechnology Advances

journal homepage: www.elsevier.com/locate/biotechadv

Research review paper

Flavoprotein monooxygenases: Versatile biocatalysts

Caroline E. Paul^a, Daniel Eggerichs^b, Adrie H. Westphal^c, Dirk Tischler^b, Willem J. H. van Berkel^{d,*}

^a Biocatalysis, Department of Biotechnology, Delft University of Technology, Van der Maasweg 9, 2629 HZ Delft, The Netherlands

^b Microbial Biotechnology, Faculty of Biology and Biotechnology, Ruhr-Universität Bochum, Universitätsstrasse 150, 44780 Bochum, Germany

^c Laboratory of Biochemistry, Wageningen University, Stippeneng 4, 6708 WE Wageningen, The Netherlands

^d Laboratory of Food Chemistry, Wageningen University, Bornse Weiland 9, 6708 WG Wageningen, The Netherlands

ARTICLE INFO

Keywords:

Baeyer-Villiger oxidation
biocatalysis
dearomatization
epoxidation
flavin
halogenation
hydroxylation
oxygenation
(hydro)peroxide
microbial degradation

ABSTRACT

Flavoprotein monooxygenases (FPMOs) are single- or two-component enzymes that catalyze a diverse set of chemo-, regio- and enantioselective oxyfunctionalization reactions. In this review, we describe how FPMOs have evolved from model enzymes in mechanistic flavoprotein research to biotechnologically relevant catalysts that can be applied for the sustainable production of valuable chemicals. After a historical account of the development of the FPMO field, we explain the FPMO classification system, which is primarily based on protein structural properties and electron donor specificities. We then summarize the most appealing reactions catalyzed by each group with a focus on the different types of oxygenation chemistries. Wherever relevant, we report engineering strategies that have been used to improve the robustness and applicability of FPMOs.

1. Introduction

Flavoprotein monooxygenases (FPMOs) are involved in a variety of biological processes ranging from lignin degradation to the biosynthesis of natural products and detoxification of xenobiotic compounds (Huijbers et al., 2014). FPMOs are redox enzymes that use a flavin mononucleotide (FMN) or flavin adenine dinucleotide (FAD) cofactor to activate dioxygen (O_2) (Massey, 1994; Romero et al., 2018). They catalyze the incorporation of one atom of O_2 into a substrate and the reduction of the other oxygen atom to water. O_2 activation by FPMOs typically proceeds through covalent adduct formation between the two-electron reduced flavin cofactor and the O_2 molecule. Most FPMOs thus (transiently) stabilize the canonical flavin C4a-(hydro)peroxide oxygenation species, which can in turn, depending on its protonation state, perform a nucleophilic or electrophilic attack on the substrate (Fig. 1a) (Massey, 1994). Recent studies have indicated that in certain FPMOs, O_2 activation involves an adduct formation via the flavin N5 (Fig. 1b), and that this mode of activation might be more general than previously anticipated (Beaupre and Moran, 2020; Matthews et al., 2020).

NMR studies have indicated that the N1 of the isoalloxazine ring of

the reduced flavin in most flavoenzymes has a lower pKa than that of free reduced FMN (pKa = 6.7) (Müller, 2014). Therefore, it can be assumed that for FPMOs (usually having pH optima around 8), the N1 of the reduced flavin is anionic. Thus, for simplicity, we have drawn the anionic reduced flavin in all figures.

Table 1 presents an overview of milestones in the FPMO field. The first purified FPMO, lactate 2-monooxygenase (LaMO; EC 1.13.12.4), was reported in 1954 (Sutton, 1954, 1955, 1957). In the following decades, newly discovered FPMOs were mainly studied for their role in the biodegradation of natural and xenobiotic compounds (Harwood and Parales, 1996; Ziegler, 1988) and for their mode of oxygen activation (Massey, 1994; Müller, 1985, 1987). Thanks to the colorful absorbance and fluorescence properties of the flavin cofactor and the fact that the reductive and oxidative half-reactions of FPMOs can be separately monitored in the absence or presence of O_2 , the kinetic properties and catalytic mechanisms of these redox enzymes can be conveniently studied by stopped-flow spectroscopic techniques. This resulted in 1976 in a detailed description of the catalytic cycle of 4-hydroxybenzoate 3-hydroxylase from *Pseudomonas fluorescens* (PHBH; EC 1.14.13.2; Fig. 4) (Entsch et al., 1976).

PHBH also became the first FPMO for which a crystal structure was

* Corresponding author.

E-mail address: willem.vanberkel@wur.nl (W.J.H. van Berkel).

<https://doi.org/10.1016/j.biotechadv.2021.107712>

Received 13 November 2020; Received in revised form 27 January 2021; Accepted 6 February 2021

Available online 13 February 2021

0734-9750/© 2021 The Authors. Published by Elsevier Inc. This is an open access article under the CC BY license (<http://creativecommons.org/licenses/by/4.0/>).

elucidated (Fig. 2) (Wierenga et al., 1979). Intriguingly, completion of the primary structure determination of PHBH via Edman degradation took another three years (Weijer et al., 1983; Weijer et al., 1982). In 1990, about 30 FPMOs had been isolated and (partially) characterized (van Berkel and Müller, 1991), whereas high-resolution crystal structures of wild-type enzyme (Schreuder et al., 1989) and an engineered variant (Eschrich et al., 1990) were only available for PHBH. Most of the FPMOs known at that time had a narrow substrate scope, and relatively little attention was paid to their synthetic potential. The first FPMO with exquisite versatility in terms of type of reaction, substrate scope and attractive regiochemistry was reported in 1985 (Branchaud and Walsh, 1985; Taschner and Black, 1988; Walsh and Chen, 1988). This Baeyer-Villiger monooxygenase (BVMO), i.e. cyclohexanone monooxygenase from *Acinetobacter* sp. NCIMB 9871 (CHMO; EC 1.14.13.22), had already been purified in 1976 (Donoghue et al., 1976), but it took 33 years before the first crystal structure of a CHMO, i.e. CHMO from *Rhodococcus* sp. strain HI-31, became available (Mirza et al., 2009).

Around the turn of the century, the interest in the application of FPMOs for the production of valuable chemicals was boosted by the developments in recombinant DNA technology and the accompanying improvements in enzyme production, enzyme purification and enzyme engineering. As a result, several new FPMOs were discovered and analyzed for their biochemical, structural and biocatalytic properties (Fraaije and van Berkel, 2006). This allowed for a first classification of FPMOs based on the properties of 65 different enzymes (van Berkel et al., 2006). In 2014, the number of characterized FPMOs had doubled again, and more than 130 different enzymes could be distributed into eight groups (Huijbers et al., 2014). In the past few years, many new FPMOs have been discovered, especially in the context of the biosynthesis of natural products (Tang et al., 2017; Walsh and Wenciewicz, 2013) and unearthing new oxidative biocatalysts for applications in the pharmaceutical industry (Fürst et al., 2019c). Currently, the FPMO family comprises approximately 300 enzymes for which the physiological function is known. For several other members, discovered by genome mining, the biological function remains unclear. Nevertheless, many of them have been crystallized, which raises the number of solved FPMO structures far over one hundred. The search for new FPMOs has also contributed to new insights in the mode of action of FPMOs. Detailed information about mechanistic features of FPMOs can be found in recent reviews (Adak and Begley, 2017a; Beaupre and Moran, 2020; Chenprakhon et al., 2019; Fürst et al., 2019b; Gassner, 2019; Piano

et al., 2017; Robbins and Ellis, 2019; Romero et al., 2018; Saleem-Batcha et al., 2018; Tolmie et al., 2019; Toplak et al., 2021). Here we focus on the classification of FPMOs and the biotechnological most appealing reactions within each group.

2. FPMO classification

The first classification of FPMOs was published in 2006 (van Berkel et al., 2006). Based on distinct structural and functional properties, FPMOs were divided into six groups including single-component enzymes that use nicotinamide adenine (phosphorylated) dinucleotide NAD(P)H as external electron donor (group A and B) and two-component enzymes that use a flavin reductase for electron supply (group C to F, Table 2). In 2014, group G and H were added, which comprise self-sufficient ('internal') FPMOs, that do not need an external electron donor (Table 2) (Huijbers et al., 2014).

Group A FPMOs act mainly as aromatic hydroxylases. They contain a Rossmann-like three-layer $\beta\beta\alpha$ sandwich domain for binding the FAD cofactor (CATH code 3.50.50.60) and a β -strand rich substrate domain (CATH code 3.30.9.10, Fig. 2). Group A members display flavin mobility (Entsch and van Berkel, 1995), bind the NAD(P)H coenzyme in a groove at the protein surface (Westphal et al., 2018), and can be distinguished from other FAD-dependent FPMOs by their conserved FAD-NAD(P)H binding motif (DG fingerprint) (Eppink et al., 1997). Another distinct feature of group A FPMOs is the effector role of the substrate, which stimulates flavin reduction and NAD(P)⁺ release (Ballou and Entsch, 2013).

Group B FPMOs represent mainly Baeyer-Villiger monooxygenases (Type I BVMOs) and heteroatom oxygenases. These enzymes also contain a Rossmann-like three-layer $\beta\beta\alpha$ sandwich domain for FAD binding, but do not contain a specific substrate domain (Fig. 2). They bind the substrate after flavin reduction and NAD(P)⁺ remains bound during substrate oxidation (Ballou and Entsch, 2013; Romero et al., 2018). In order to do so, group B enzymes contain a separate three-layer $\beta\beta\alpha$ sandwich domain for binding the pyridine nucleotide (Fig. 2) (Alferi et al., 2008; Malito et al., 2004).

Group C to F FPMOs act in concert with a flavin reductase. They usually bind the reduced flavin much stronger than oxidized flavin. Flavin transfer from the reductase to the monooxygenase may require a certain interaction between the protein partners, but generally occurs through free diffusion (Sucharitakul et al., 2014).

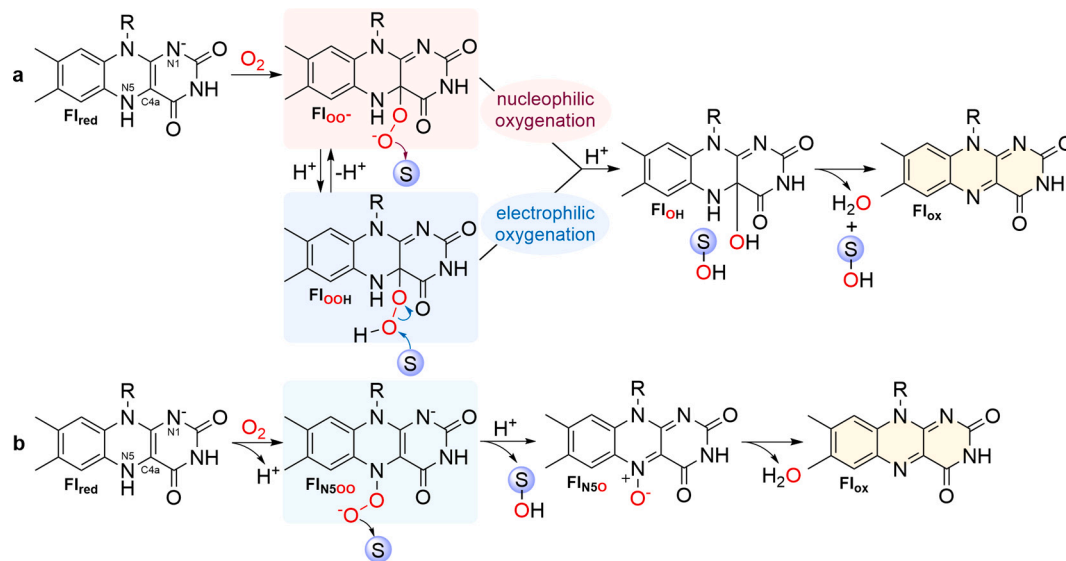


Fig. 1. Covalent flavin-oxygen adducts of FPMOs. a) Reaction of reduced flavin (Fl_{red}) and O₂ leads to flavin C4a-(hydro)peroxide (Fl_{OO(H)}), which reacts with a substrate (S) to form product (SOH) and flavin C4a-hydroxide (Fl_{OH}). Fl_{OH} decays, upon release of water, to oxidized flavin (Fl_{ox}). b) Reaction of Fl_{red} and O₂ leads to flavin N5-peroxide (Fl_{N5OO}), which reacts with the substrate to form product SOH and flavin N5-oxide (Fl_{N5O}).

Group C FPMOs catalyze different types of oxygenation reactions. They share a luciferase-like TIM-barrel fold for binding FMNH₂ (Fig. 2) (Ellis, 2010). This group contains inter alia pyrimidine monooxygenase (RutA; EC 1.14.99.46 (Adak and Begley, 2017b)), dibenzothiophene sulfone monooxygenase (DszA (Adak and Begley, 2016; Mohamed et al.,

2015)) and hexachlorobenzene monooxygenase (HcbA1 (Adak and Begley, 2019b)), which have been proposed to form a flavin N5-(per)oxide intermediate (Adak and Begley, 2019a; Matthews et al., 2020).

Group D FPMOs also catalyze a motley collection of oxygenation reactions. They either accept FMNH₂ or FADH₂ or both, and have an

Table 1

Milestones in FPMO research.

Milestones in FPMO research.

Year	Milestone	Reference
1954	First purified internal FPMO (LaMO)	(Sutton, 1954, 1955)
1961	First two-component FPMO (2,5-DKCMO)	(Conrad et al., 1961)
1965	First purified external FPMO (SalH)	(Yamamoto et al., 1965)
1972	Purification of pig liver FMO	(Ziegler and Mitchell, 1972)
1972	First purified FAD-requiring epoxidase (SQLE)	(Tai and Bloch, 1972)
1976	First purified type I BVMO (CHMO)	(Donoghue et al., 1976)
1976	Catalytic mechanism PHBH	(Entsch et al., 1976)
1979	First (partial) purification of NMO	(Parniak et al., 1979)
1979	First FPMO 3D-structure (PHBH)	(Wierenga et al., 1979)
1981	Catalytic mechanism pig liver FMO	(Beaty and Ballou, 1981a, b)
1982	Catalytic mechanism CHMO	(Ryerson et al., 1982)
1982	First FPMO amino acid sequence (PHBH)	(Weijer et al., 1982)
1984	Oxygen-flavin chemistry	(Bruce, 1984)
1985	First versatile FPMO biocatalyst (CHMO)	(Branchaud and Walsh, 1985)
1986	NMR evidence flavin-C4a-peroxide (LUX)	(Vervoort et al., 1986)
1988	First FPMO DNA sequence (CHMO)	(Chen et al., 1988)
1990	First 3D-structure of a recombinant FPMO (PHBH)	(Eschrich et al., 1990)
1994	Flavin mobility (PHBH)	(Schreuder et al., 1994)
1995	First 3D-structure of a two-component FPMO (LUX)	(Fisher et al., 1995)
1996	First purified enantiocomplementary FPMOs (2,5-DKCMO and 3,6-DKCMO)	(McGhie and Littlechild, 1996)
1997	Flavoprotein hydroxylase sequence motif	(Eppink et al., 1997)
1998	First crystallization type II BVMO (3,6-DKCMO)	(McGhie et al., 1998)
2000	First flavin-dependent halogenase (PrnA)	(Keller et al., 2000)
2001	First gram scale biocatalytic production of chiral styrene oxides (SMO)	(Schmid et al., 2001)
2002	Pilot scale biocatalytic production of chiral styrene oxide (SMO)	(Panke et al., 2002)
2002	BVMO sequence motif	(Fraaije et al., 2002)
2004	First 3D-structure of a type I BVMO (PAMO)	(Malito et al., 2004)
2005	First 3D-structure of a flavin-dependent halogenase (PrnA)	(Dong et al., 2005)
2005	First kilogram scale asymmetric Baeyer-Villiger oxidation (CHMO)	(Hilker et al., 2005)
2006	First classification FPMOs (groups A-F)	(van Berkel et al., 2006)
2007	Genome mining FPMOs (SMO-A)	(van Hellemond et al., 2007)
2007	First 3D-structure of a group D FPMO (C2-HpaH)	(Alfieri et al., 2007)
2008	First 3D-structure of an internal FPMO (PAO)	(Ida et al., 2008)
2008	Catalytic mechanism of group D FPMO (C2-HpaH)	(Sucharitakul et al., 2008)
2009	Oxygen diffusion (C2-HpaH)	(Baron et al., 2009)
2009	First self-sufficient SMO (StyA2B)	(Tischler et al., 2009)
2010	First 3D-structure of a group E FPMO (SMO-A)	(Ukaegbu et al., 2010)
2010	Flavin radical mechanism of NiMO	(Gadda and Francis, 2010)
2011	Enzymatic synthesis of esomeprazole (CHMO)	(Bong et al., 2011)
2012	FPMO-mediated oxidative dearomatization (TropB)	(Davison et al., 2012)
2013	Flavin N5-oxide (EncM)	(Teufel et al., 2013)
2014	Classification of FPMOs group A-H	(Huijbers et al., 2014)
2014	First 3D-structure of a group H FPMO (NiMO)	(Salvi et al., 2014)
2015	First 3D-structure of a type II BVMO (3,6-DKCMO)	(Isupov et al., 2015)
2015	First gram scale halogenation (RebH)	(Frese and Sewald, 2015)
2016	FPMO evolution	(Mascotti et al., 2016)
2017	First kilogram scale chiral sulfoxide drug intermediate (BVMO)	(Goundry et al., 2017)
2017	Total synthesis bisorbicillinoid natural products (SorbC)	(Sib and Gulder, 2017)
2018	First 3D-structure insect FMO (ZvPNO)	(Kubitza et al., 2018)
2019	First whole-cell gram scale oxidative dearomatization of phenols (TropB)	(Baker Dockrey et al., 2019)
2020	Flavin N5-peroxide (RutA)	(Matthews et al., 2020)
2020	First 3D-structures of human FMOs	(Nicoll et al., 2020)
2020	First 3D-structure of a plant FPMO (AsFMO)	(Valentino et al., 2020)

Milestones are colored according to enzyme discoveries (orange), mechanistic progress (white), protein structure determinations (blue), and biocatalytic developments (yellow).

Milestone references not cited in text: Alfieri et al., 2007; Baron et al., 2009; Beaty and Ballou, 1981a; Beaty and Ballou, 1981b; Bruce, 1984; Chen et al., 1988; Fraaije et al., 2002; Goundry et al., 2017; Hilker et al., 2005; Parniak et al., 1979; Schreuder et al., 1994; Sucharitakul et al., 2008; van Hellemond et al., 2007; Vervoort et al., 1986

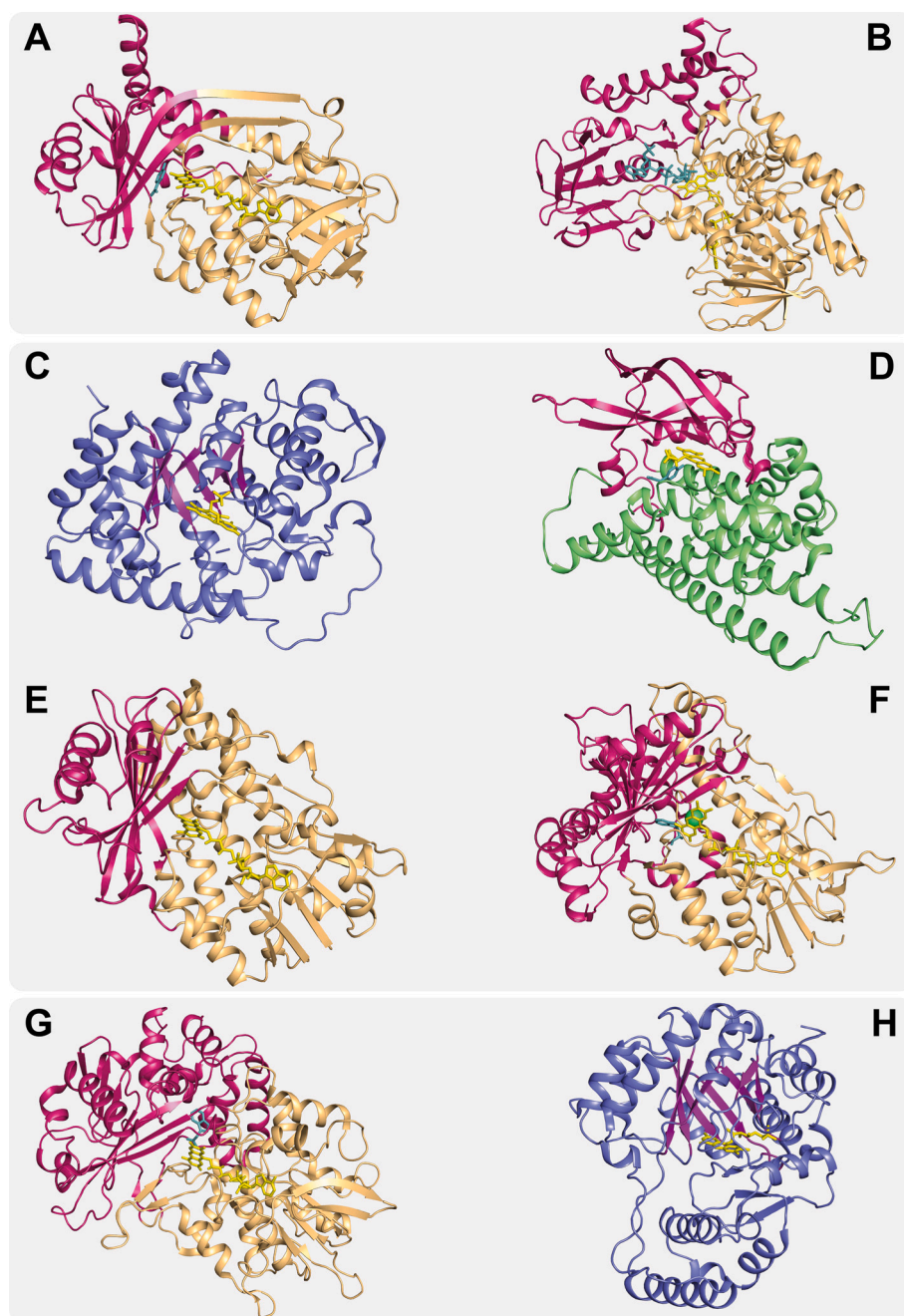


Fig. 2. Crystal structures of FPMOs group A to H. External FPMOs (A and B), two-component FPMOs (C to F), internal FPMOs (G and H). Protein Data Bank (PDB) number used in brackets. (A) 4-hydroxybenzoate 3-hydroxylase (PHBH; 1pbe); (B) phenylacetone monooxygenase (PAMO; 2ym2); (C) bacterial luciferase (1luc); (D) 4-hydroxyphenylacetate 3-hydroxylase (HpaB; 2jbt); (E) styrene monooxygenase (StyA; 3ihm); (F) tryptophan 7-halogenase (PrnA; 2aqj); (G) tryptophan 2-monooxygenase (4iv9); (H) nitronate monooxygenase (NiMO; 6bka). FAD binding domains are colored yellow-orange, TIM-barrel-containing proteins in blue with β -strands of the TIM-barrel in purple, acyl-CoA dehydrogenase domain in green, substrate binding domains in dark pink, FAD/FMN in yellow and (co-)substrates in grey-blue. (For interpretation of the references to color in this figure legend, the reader is referred to the web version of this article.)

Table 2
Classification of FPMOs.

Group	Flavin-binding domain	CATH code	Cofactor	Electron donor	Prototype reaction
A	three-layer $\beta\beta\alpha$ sandwich	3.50.50.60	FAD	NAD(P)H	aromatic hydroxylation
B	three-layer $\beta\beta\alpha$ sandwich	3.50.50.60	FAD	NAD(P)H	Baeyer-Villiger oxidation
C	TIM-barrel	3.20.20.30	FMN	FMNH ₂	light emission
D	acyl-CoA dehydrogenase	1.10.540.10	FAD/FMN	FADH ₂ /FMNH ₂	aromatic hydroxylation
E	three-layer $\beta\beta\alpha$ sandwich	3.50.50.60	FAD	FADH ₂	epoxidation
F	three-layer $\beta\beta\alpha$ sandwich	3.50.50.60	FAD	FADH ₂	oxidative halogenation
G	three-layer $\beta\beta\alpha$ sandwich	3.50.50.60	FAD	Substrate	oxidative deamination
H	TIM-barrel	3.20.20.70	FMN	Substrate	oxidative decarboxylation

Groups are colored based on the CATH (Class, Architecture, Topology and Homologous superfamily) classification of their flavin binding domain (Mascotti et al., 2016) (cf. Fig 2).

acyl-CoA dehydrogenase fold (Fig. 2) (Chenprakhon et al., 2019).

Group E and F FPMOs comprise epoxidases and halogenases, respectively (Heine et al., 2018). They resemble group A members in having a three-layer $\beta\alpha$ sandwich domain (Fig. 2), but differ in their C-terminal sequences (Mascotti et al., 2016; Montersino et al., 2011).

Group G and H FPMOs are single-component enzymes that reduce the flavin cofactor through substrate oxidation. They mainly catalyze oxidative deamination and oxidative decarboxylation reactions. Group G enzymes contain in addition to a three-layer $\beta\alpha$ sandwich domain a monoamine oxidase like domain (CATH 3.90.660.10) and a C-terminal α -helix domain (Fig. 2). Group H enzymes on the other hand contain a type I aldolase-like TIM-barrel domain for binding FMN (Fig. 2) (Huijbers et al., 2014).

The flavin N5-oxide stabilizing enterocin biosynthesis mono-oxygenase (EncM) is a new type of FPMO. EncM contains a VAO/PCMH fold (Ewing et al., 2017) and binds its FAD cofactor in a covalent mode (Teufel et al., 2013). EncM, not further discussed here, represents an “inverted internal FPMO” since it catalyzes oxygenation first (enabled by the stable N5-oxide) before substrate dehydrogenation takes place (Teufel et al., 2015; Toplak et al., 2021).

3. FPMO-catalyzed reactions

FPMOs catalyze a remarkable diverse set of chemo-selective oxygenation reactions. Groups A to D show a high diversity in oxygenation chemistries, whereas groups E to H are far more specific in the type of reactions they catalyze (Fig. 3). Interestingly, it is only in a few cases that a certain type of oxygenation reaction is linked to a specific fold.

3.1. Group A reactions

Group A constitutes the largest group of the FPMO family. Up to now,

approximately 90 members have been (partially) characterized. Most of them catalyze the monooxygenation of an electron-rich aromatic substrate using the flavin C4a-hydroperoxide as electrophile (Fig. 1, Fig. 4). Depending on the enzyme, a proton or another leaving group is then abstracted from the aromatic ring resulting in a hydroxylated aromatic compound in which the hydroxy group either replaces another functional moiety (*ipso*-substitution) or is newly introduced (hydroxylation, Fig. 4a). Alternatively, a quinol can be formed if the hydroxylation takes place at an alkylated carbon atom in *ortho*-position to another hydroxy group (dearomatization, Fig. 4b). Furthermore, a subgroup of group A enzymes catalyzes epoxidation reactions (*vide infra*, Fig. 4e).

Many group A enzymes catalyze the regioselective hydroxylation of activated aromatic compounds, including among others anilines, benzoquinones, indoles, phenazines, phenols, phytoalexins and polyketides (Fig. 4). Each enzyme accepts a limited number of substrates and catalyzes either a *para*- or *ortho*-hydroxylation reaction. This leads to the interesting observation that certain group A enzymes react with the same substrate but form a different product, such as 3-hydroxybenzoate 4-hydroxylase (3HB4H; EC 1.14.13.23 (Hiromoto et al., 2006)) and 3-hydroxybenzoate 6-hydroxylase (3HB6H; EC 1.14.13.24 (Montersino et al., 2013)). A unique situation is observed in ubiquinone biosynthesis. Here, multiple proteobacterial group A enzymes with various regioselectivities (UbiF, UbiH, UbiI; EC 1.14.13.240, UbiL and UbiM) have evolved to catalyze three contiguous hydroxylation reactions (Pelosi et al., 2016). Being omnipresent in microbial degradation pathways (Nakamoto et al., 2019; Yu et al., 2018), group A hydroxylases convert a wide variety of monocyclic aromatic compounds. In contrast, during the biosynthesis of complex natural products like fungal alkaloids, group A enzymes tend to convert large substrates like polyketides with a remarkable regioselectivity (Fig. 4e-f).

Fig. 4 shows the catalytic cycle of PHBH, the prototype of group A, and a simplified scheme of its oxygenation mechanism (Entsch and van

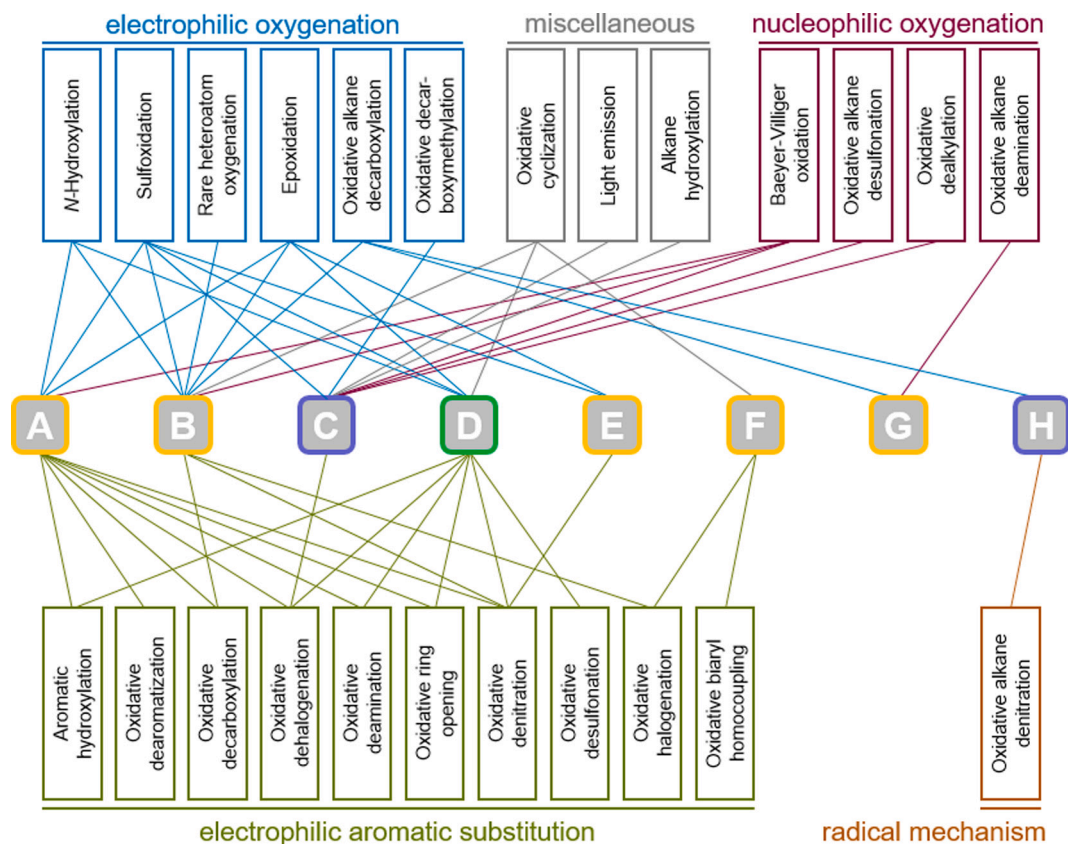


Fig. 3. Schematic representation of reactions catalyzed by FPMOs, ordered by the underlying reaction type mechanism. Enzyme groups A to H are framed according to the color of their flavin-binding domain (cf. Table 2 and Fig. 2).

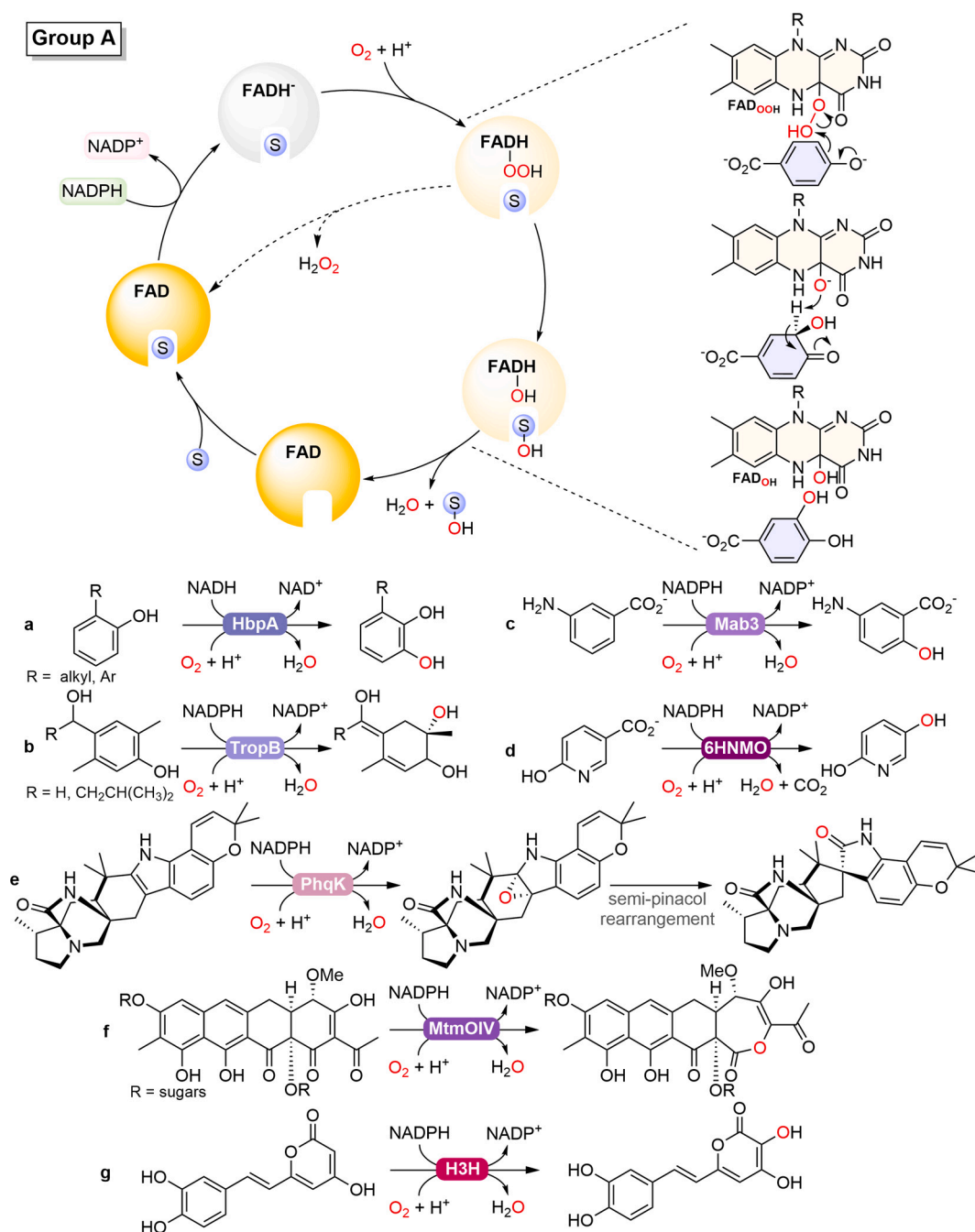


Fig. 4. Catalytic cycle of group A FPMOs. Top: The oxygenation reaction proposed for PHBH from *Pseudomonas fluorescens* is depicted. The side reaction of hydrogen peroxide formation was not observed for PHBH but is common for other group A members. Bottom: Overview of the substrate scope of group A enzymes. a) Hydroxylation of substituted phenolic compounds to substituted catechols by HbpA from *Pseudomonas azelaica* HBP1; b) Oxidative dearomatization of substituted phenols to cyclic chiral dienones by TropB from *Talaromyces stipitatus*; c) Hydroxylation of 3-aminobenzoate to 5-amino-2-hydroxybenzoate by Mab3 from *Comamonas testosteroni*; d) Oxidative decarboxylation of 6-hydroxynicotinate to 2,5-dihydroxypyridine by 6HNMO from *Pseudomonas fluorescens* TN5; e) Epoxidation of the indole alkaloid paraherquamide K to the indole oxide followed by a semi-pinacol rearrangement by spirocycle-forming flavin monooxygenase PhqK from *Penicillium simplicissimum*; f) Baeyer-Villiger oxidation of premithramycin B to premithramycin B lactone by MtmOIV from *Streptomyces argillaceus*; g) Hydroxylation of hispidin to 3-hydroxyhispidin (fungal luciferin) by hispidin 3-hydroxylase H3H from *Mycena chlorophos*.

Berkel, 1995). PHBH from *Pseudomonas fluorescens* is one of the few group A enzymes that does not produce hydrogen peroxide as by-product. This shunt pathway (Fig. 4) occurs when the flavin C4a-hydroperoxide intermediate is not sufficiently stabilized. Deprotonation of 4-hydroxybenzoate to its dianionic form is necessary for flavin reduction and efficient substrate hydroxylation, and is facilitated by an extended hydrogen bond network that runs from the substrate binding pocket to the protein surface (Palfey et al., 1999).

As noted above, certain group A enzymes can catalyze sequential hydroxylation reactions. Early mutagenesis studies of PHBH established that in contrast to wild-type enzyme, the active site variant Y385F stimulates the further hydroxylation of the aromatic product 3,4-dihydroxybenzoate (protocatechuic acid) to 3,4,5-trihydroxybenzoate (gallic acid) (Entsch and van Berkel, 1995). For the alternative substrate tetrafluoro-4-hydroxybenzoate, it could be demonstrated that Y385F generates, besides 2,6-difluoro-3,4,5-trihydroxybenzoate, significant

amounts of 5,6-difluoro-2,3,4-trihydroxybenzoate and 5-fluoro-tetrahydroxybenzoate (van der Bolt et al., 1997). More recently, this concept was used to increase the amount of gallic acid from protocatechuate by creating the double mutants Y385F/T294A (Chen et al., 2017) and Y385F/L199V (Moriwaki et al., 2019).

The exquisite regioselectivity of group A enzymes has attracted interest for biocatalytic applications. 2-Hydroxybiphenyl 3-mono-oxygenase (HbpA; EC 1.14.13.44) has been used to generate a wide range of substituted catechols with aliphatic or aromatic side chains (Fig. 4a) (Bregman-Cohen et al., 2018; Lutz et al., 2002; Meyer et al., 2002). Another promising enzyme is 3-aminobenzoate 6-hydroxylase (Mab3), which catalyzes the *para*-hydroxylation of 3-aminobenzoate to 2-hydroxy-5-aminobenzoate (5-aminosalicylate, mesalazine; Fig. 4c), a medication for the treatment of inflammatory bowel disease (Yu et al., 2018). Hispidin 3-hydroxylase (H3H) catalyzes the hydroxylation of the 6-hydroxypyran-4-one moiety of hispidin yielding 3-hydroxyhispidin (Fig. 4g), which acts as luciferin substrate in luminescent fungi (Kaskova et al., 2017; Kotlobay et al., 2018). H3H was recently biochemically characterized and its coenzyme preference was changed from NADPH to NADH by site-directed mutagenesis (Tong et al., 2020).

An important hydroxylation reaction catalyzed by several group A enzymes concerns the *ipso*-attack described above (Ricken et al., 2015). In such reaction, the entering hydroxyl attaches to a position in the aromatic ring already carrying a substituent, and this substituent can either expel or migrate in a subsequent step. Classic examples concern salicylate 1-hydroxylase (SalH; EC 1.14.13.1; (Costa et al., 2019; Yamamoto et al., 1965)) and 6-hydroxynicotinate 3-mono-oxygenase (6HNMO; EC 1.14.13.114; Fig. 4d (Nakano et al., 1999)), catalyzing oxidative decarboxylation reactions.

Using the *ipso* mechanistic pathway, an exciting property of certain group A enzymes is the stereoselective oxidative dearomatization giving access to substituted *ortho*-quinols, including oxidative cyclization products (Abood et al., 2015; Baker Dockrey et al., 2018; Baker Dockrey and Narayan, 2020; Milzarek et al., 2019; Rodríguez Benítez et al., 2019; Sib and Gulder, 2017; Tang et al., 2017). This type of reaction is catalyzed by TropB (3-methylcinnamaldehyde mono-oxygenase; Fig. 4b), SorbC ((dihydro)sorbicillin mono-oxygenase) and AzaH (azaphilone biosynthesis mono-oxygenase) (Al Fahad et al., 2014; Davison et al., 2012; Zabala et al., 2012). These oxidative dearomatizations have enabled access to the synthesis of a variety of sorbicillinoid derivatives by SorbC (Sib and Gulder, 2017, 2018; Sib et al., 2019) and substituted chiral building blocks for natural products on a gram scale by TropB (Baker Dockrey et al., 2019).

Some group A enzymes catalyze Baeyer-Villiger oxidations and are referred to as atypical type O BVMOs. They are especially found in complex biosynthetic pathways of secondary metabolites such as polyether antibiotics in *Streptomyces* species (Tolmie et al., 2019). The first representative is premithramycin B mono-oxygenase (MtmOIV) from *Streptomyces argillaceus* ATCC 12956 (Beam et al., 2009; Gibson et al., 2005). MtmOIV catalyzes a Baeyer-Villiger oxidation on premithramycin B (heavily glycosylated multi-cyclic core) towards the corresponding lactone (Fig. 4f) (Bosserman et al., 2013). The related rifampicin mono-oxygenase (RIFMO or Rox; EC 1.14.13.211) from *Streptomyces venezuela* was shown to catalyze the hydroxylation of position 2 of the naphthyl group of rifampicin, which leads to a ring opening and thus inactivates the antibiotic (Koteva et al., 2018). The crystal structure of the enzyme-product complex of RIFMO from *Nocardia farcinica* has provided strong support for this mechanism (Liu et al., 2016; Liu et al., 2018). RIFMO displays a similar fold and quaternary structure to MtmOIV and 5a,11a-dehydrotetracycline-5-mono-oxygenase from *Streptomyces rimosus* (OxyS; EC 1.14.13.234), enzymes involved in the mithramycin and oxytetracycline biosynthetic pathways, respectively (Bosserman et al., 2013; Liu et al., 2016; Wang et al., 2013).

Several group A FPMOs catalyze epoxidation reactions. Squalene epoxidase (SQLE; EC 1.14.13.132) represents the first described FPMO with epoxidase activity (Table 1) (Tai and Bloch, 1972). Eukaryotic

SQLE catalyzes the conversion of squalene to (3S)-2,3-oxidosqualene, which is a rate-limiting step of cholesterol biogenesis (Sakakibara et al., 1995). Zeaxanthin epoxidase (ZEP; EC 1.14.13.90) is present in plants and converts zeaxanthin via antheraxanthin to violaxanthin (Buch et al., 1995). Being membrane associated, SQLE and ZEP receive their reducing equivalents from electron-transfer protein complexes and not from free NAD(P)H. A crystal structure of the catalytic domain of SQLE was recently obtained (Brown et al., 2019; Padyana et al., 2019), which might stimulate future biocatalytic applications. Further examples of group A epoxidases include FPMOs from *Streptomyces* species, which catalyze sequential enantioselective epoxidations during the biosynthesis of polyether antibiotics (Minami et al., 2013), and several recently characterized diastereoselective FPMOs involved in fungal indole alkaloid biosynthesis (Fraley et al., 2020; Fraley and Sherman, 2020; Matsushita et al., 2020). As an example, the conversion of paraherquamide K catalyzed by the spirocycle-forming mono-oxygenase PhqK from *P. simplicissimum* is depicted in Fig. 4e.

3.2. Group B

Group B FPMOs comprise several distinct subgroups, including Baeyer-Villiger mono-oxygenases (BVMOs; subgroup B1), flavin-containing mono-oxygenases (FMOs; subgroup B2) and *N*-hydroxylating mono-oxygenases (NMOs; subgroup B3) (van Berkel et al., 2006). This original subgroup classification was later supported by phylogenetic studies (Mascotti et al., 2015; Riebel et al., 2013).

Subgroup B1 consists of microbial NADPH-dependent BVMOs. These FAD-containing enzymes, usually referred to as type I BVMOs, catalyze the enantioselective conversion of a wide range of ketones to esters or lactones (Fig. 5) (Alphand et al., 2003; Kamerbeek et al., 2003; Schwab, 1981; Stewart, 1998). Type I BVMOs can also react with aldehydes, thereby forming either acids or formate derivatives (Ferroni et al., 2017; Leisch et al., 2011; Moonen et al., 2005).

The catalytic cycle of type I BVMOs, as first established for CHMO, is depicted in Fig. 5 (Ryerson et al., 1982; Sheng et al., 2001). Catalysis is initiated by flavin reduction through the NADPH co-substrate. After oxygen activation of the reduced enzyme-NADP⁺ complex, the substrate binds and is converted to a tetrahedral Criegee intermediate by means of a nucleophilic attack of the anionic flavin C4a-peroxide on the carbonyl group. This intermediate undergoes a rearrangement involving migration of one of the substituents of the carbonyl carbon and subsequent heterolytic cleavage of the peroxidic bond yielding the ester or lactone and flavin C4a-hydroxide. After product release, the flavin C4a-hydroxide decomposes to oxidized flavin and finally, NADP⁺ and water are released.

Phenylacetone mono-oxygenase (PAMO; EC 1.14.13.92) was the first type I BVMO with a known 3D-structure (Malito et al., 2004). This milestone (Table 1) gave a huge boost to the BVMO research, and led to a strong increase in the number of studies about their biocatalytic properties (Baldwin et al., 2008; Balke et al., 2012; Bucko et al., 2016; Catucci et al., 2017; de Gonzalo et al., 2010; Leisch et al., 2011; Messiha et al., 2018; Schmidt and Bornscheuer, 2020; Sole et al., 2019; Torres Pazmiño et al., 2010). Since 2004, many new members were discovered and characterized (Fraaije et al., 2005; Mascotti et al., 2013; Riebel et al., 2012; Romero et al., 2016), and different protein engineering approaches were implemented for improving the cofactor regeneration, substrate scope and thermal stability of BVMOs (Dudek et al., 2014; Fürst et al., 2019a; Fürst et al., 2019b; Fürst et al., 2019c; Fürst et al., 2018; Fürst et al., 2017; Li et al., 2017; Li et al., 2018; Opperman and Reetz, 2010; Reetz, 2009; Reetz and Wu, 2008, 2009; van Beek et al., 2012; Wu et al., 2010).

The outstanding BVMO activity of subgroup B1 distracts often from the other reaction types performed by members of this group. A remarkable improvement in catalytic performance and operational stability was achieved with the CHMO-mediated sulfoxidation of pyrimetazole, yielding the gastric acid inhibitor esomeprazole (Fig. 5i)

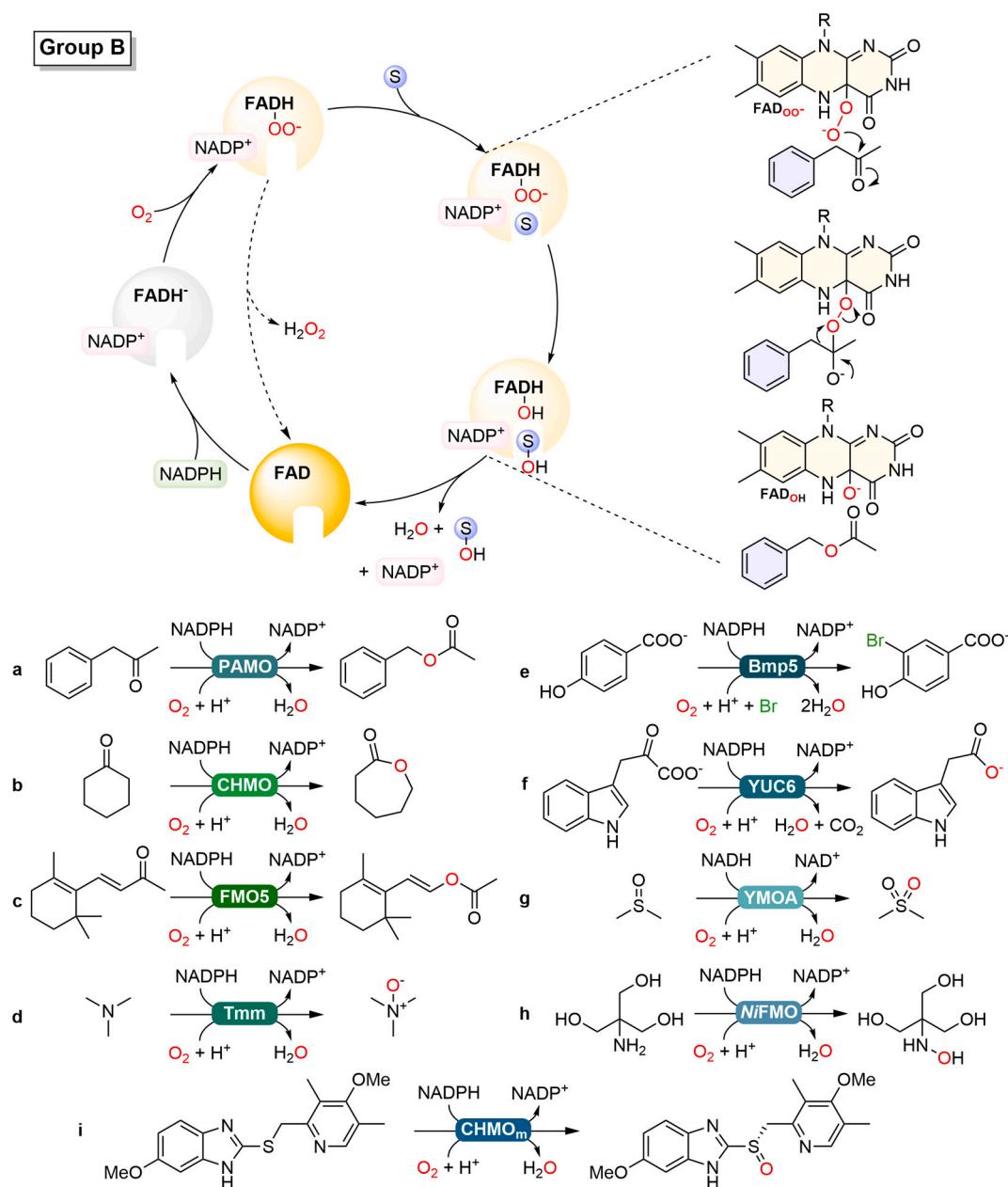


Fig. 5. Catalytic cycle of group B FPMOs. Top: The oxygenation reaction proposed for PAMO from *Thermobifida fusca* is depicted. Bottom: Overview of the substrate scope of group B enzymes. a) Baeyer-Villiger oxidation of phenylacetone to benzyl acetate by PAMO; b) Baeyer-Villiger oxidation of cyclohexanone to ϵ -caprolactone by CHMO from *Acinetobacter* sp. NCIB 9871; c) Baeyer-Villiger oxidation of β -ionone to its acetate by flavin-containing monooxygenase FMO5 from human; d) *N*-hydroxylation of trimethylamine to trimethylamine *N*-oxide by flavin-containing monooxygenase Tmm found in marine bacterial metagenome; e) Halogenation of 4-hydroxybenzoate to 3-bromo-4-hydroxybenzoate by Bmp5 from *Pseudoalteromonas luteoviolacea*; f) Oxidative decarboxylation of indole-3-pyruvate to indole-3-acetic acid by YUCCA enzyme YUC6 from *Arabidopsis thaliana*; g) Sulfoxidation of dimethylsulfoxide to dimethylsulfone by YMOA from *Yarrowia lipolytica*; h) *N*-hydroxylation of tris(hydroxymethyl)aminomethane (Tris) to 2-(hydroxyamino)-2-(hydroxymethyl)propane-1,3-diol by NiFMO from *Nitriticola lacisaponeis*; i) Sulfoxidation of pyrimetazole to esomeprazole by CHMO_m from *Acinetobacter* sp. NCIB 9871.

(Bong et al., 2011; Bong et al., 2018; Xu et al., 2020; Zhang et al., 2019). CHMO is an often-employed model BVMO in biocatalytic studies. Hence, after introducing 41 amino acid replacements in different regions of the protein structure, the enzyme (CHMO_m) became far more robust and selective, resulting in an extremely high yield and enantioselectivity.

Besides *S*-oxygenations (Maczka et al., 2018), BVMOs can catalyze epoxidations (Colonna et al., 2002), *N*-oxygenations (Maczka et al., 2018), and 'rare' heteroatom oxygenations of phosphites, iodides, boronic acids and selenium compounds (Leisch et al., 2011; Walsh and Chen, 1988). Accordingly, there are, despite their name-giving-reaction, BVMOs which prefer heteroatom oxidations (Zhang et al., 2018). For the

Baeyer-Villiger monooxygenases YMOA from *Yarrowia lipolytica*, absence of BVMO activity was found, while the enzyme showed high activity for sulfoxidations of sulfides and sulfoxides (Fig. 5g). Even an activity on the common solvent dimethyl sulfoxide (DMSO) was observed and a high yield of the corresponding sulfone was obtained (Bordewick et al., 2018).

Currently, approximately 30 type I BVMOs have been investigated for their biocatalytic properties (Fürst et al., 2019c). Although the use of synthetic genes has greatly simplified the acquisition and characterization of such BVMOs, their physiological function remains in many cases unclear. Nevertheless, much effort is spent in finding new BVMOs from

extreme environments and tuning these enzymes to become suitable for industrial applications. The role of BVMOs in the microbial metabolism of natural compounds has been reviewed by Opperman and co-workers (Tolmie et al., 2019).

Subgroup B2 consists of enzymes termed flavin-containing monooxygenases (FMOs; EC 1.14.13.8). These enzymes were first discovered in mammals and humans (Ziegler and Mitchell, 1972), but are present in all kingdoms of life. With new techniques like systematic sequencing of environmental samples it was found that FMOs are abundant in heterotrophic marine bacteria where they produce the osmolyte trimethylamine-*N*-oxide by heteroatom oxygenation (Chen et al., 2011). In mammals, FMOs are responsible for the detoxification of nitrogen and sulfur-containing compounds (Cashman and Zhang, 2006; Krueger and Williams, 2005; Phillips and Shephard, 2019; Ziegler, 2002). In bacteria, also FMOs with BVMO activity were discovered (Jensen et al., 2012).

The first FMO structure, from the yeast *Schizosaccharomyces pombe*, was solved in 2006 (Eswaramoorthy et al., 2006). This structure revealed binding modes of the substrate methimazole and the NADP(H) coenzyme. The structure of FMO from *Methylophaga* sp. strain SK1 showed that FMOs resemble BVMOs in their mode of coenzyme binding and confirmed that the nicotinamide ribose of NADP⁺ is crucially involved in stabilization of the flavin oxygenation species (Alferi et al., 2008).

FMO from *Methylophaga* sp. strain SK1 was explored for its synthetic capacity and found to produce high amounts of indigo from indole (Han et al., 2008). Besides converting a series of indole derivatives into the corresponding indigoid dyes, this bacterial FMO showed moderate to good enantioselectivity in sulfoxidation reactions (Rioz-Martínez et al., 2011). The FMO from *Nitricola laciaponesis* (NIFMO) was the first to be characterized from an alkaliphile organism. This enzyme displayed thermal stability, tolerance to organic solvents, and good activity with a range of substrates (Fig. 5h; Loncar et al., 2019).

The crystal structure of pyrrolizidine alkaloid *N*-oxygenase from the grasshopper *Zonocerus variegatus* (ZvPNO) was the first FMO structure from a highly developed organism (Kubitza et al., 2018). The ZvPNO structure indicated that the overall structure of the FMO subunits has remained largely unchanged throughout evolution. It was also suggested that the substrate specificities of the three FMO isoforms present in *Z. variegatus* are dictated by the accessibility of their active sites.

Mammalian FMOs have a strong membrane association, which hampered the three-dimensional structure determination of the human isoforms for a long time, and therefore limited the understanding of the different substrate specificities of these enzymes. For instance, it remained unclear why FMO5 is the only human isoform that shows BVMO activity (Fiorentini et al., 2017). Recently, a breakthrough was achieved with the structure elucidation of three mammalian FMOs, created through ancestral-sequence reconstruction (Nicoll et al., 2020). This study highlighted the membrane binding features of the mammalian FMOs and illustrated that their substrate specificity is controlled by tunnel design rather than active-site architecture. Furthermore, it was hypothesized that the BVMO activity of FMO5 might be explained by a Glu-His switch. Another successfully crystallized ancestral FMO, derived from human FMO1, appeared to have a porous and exposed active site, allowing Baeyer-Villiger and heteroatom oxygenations with a wide range of compounds, including several drug molecules (Bailleul et al., 2021). The isoform FMO3 was produced via recombinant expression in *E. coli* cells to synthesize human drug metabolites, demonstrating the future industrial applicability of these enzymes (Catucci et al., 2020).

Plant FMOs can be divided in three clades (Schlaich, 2007). In the first clade, FMOs with NMO activity are found which are part of the biosynthetic pathway of the secondary plant metabolite pipercolate (Chen et al., 2018; Hartmann et al., 2018). This clade also harbors a fern oxime synthase (FOS1) that catalyzes the production of phenylacetaldoxime via the initial *N*-hydroxylation of phenylalanine (Thodberg et al., 2020). The second clade contains the YUCCA enzymes (EC 1.14.13.168; (Cao et al., 2019; Turnaev et al., 2020; Zhao et al., 2001),

which are involved in the biosynthesis of the multifunctional plant hormone indole-3-acetic acid (Cao et al., 2019; Mashiguchi et al., 2011). Several potent YUCCA inhibitors have been developed for the chemical genetic analysis of the different functions of the auxin phytohormone (Kakei et al., 2015; Tsugafune et al., 2017; Zhu et al., 2019). The third clade contains FMOs with sulfoxidation activity. Examples include the oxygenations of methylthioalkyl glucosinolates (Li et al., 2008) and allyl mercaptans such as alliin, produced by an FMO from *Allium sativum* (AsFMO), a precursor of allicin responsible for the characteristic smell and flavor of garlic (Valentino et al., 2020). The crystal structure of AsFMO represents the first 3D-structure of a plant FPMO (Table 1). Despite their interesting properties, plant FMOs have not yet been extensively studied for their biocatalytic potential (Thodberg and Neilson, 2020).

FMOs can also catalyze oxidative halogenation reactions. The brominase Bmp5 catalyzes two consecutive steps in the biosynthesis of polybrominated diphenyl ethers in the marine organism *Pseudoalteromonas luteoviolacea* (Agarwal et al., 2014). In the first step, 4-hydroxybenzoate is converted to 3-bromo-4-hydroxybenzoate, and this compound is subsequently transformed to 2,4-dibromophenol. Bmp5 appears to be structurally related to yeast FMO and mammalian FMO and is postulated to form flavin C4a-hydroperoxide and flavin C4a-O-Br intermediates (Teufel et al., 2016).

Subgroup B3 consists of microbial NMOs catalyzing *N*-hydroxylations of amino acids found in biosynthetic pathways of secondary metabolites like siderophores and antimicrobial agents (Ballou and Entsch, 2013; Robinson and Sobrado, 2013). Despite their close relation to the other subgroups, no sulfoxidation activity nor BVMO activity was described for NMOs so far.

The crystal structure of L-ornithine N5-monooxygenase from *Pseudomonas aeruginosa* (PvdA; EC 1.14.13.195) was the first NMO structure solved (Olucha et al., 2011). This structure revealed, next to the FAD and NADPH-binding domains, the presence of a small helical domain for binding L-ornithine. The structural properties and catalytic mechanism of NMOs, as well as their phylogeny and involvement in siderophore biosynthesis, have recently been summarized (Mügge et al., 2020). In addition, several new conformational states pointing to protein and flavin dynamics were reported for L-ornithine N5-hydroxylase from *Aspergillus fumigatus* (SidA; EC 1.14.13.196) (Campbell et al., 2020b). Based on the structural and kinetic properties of the M101A variant of SidA, it was suggested that the FAD movement from *in* to *out* in group B FPMOs is to release NADP⁺ in preparation for a new catalytic cycle (Campbell et al., 2020a).

The physiological role in the production of diazo group-containing antibiotics (Waldman et al., 2017) and other important metabolites makes NMOs interesting candidates as biocatalysts for the production of *N*-hydroxylated building blocks. One route starts with the NMO-mediated double hydroxylation of aspartate affording nitrosuccinate (Wang et al., 2018). In another route, NMO converts lysine to N6-hydroxylysine (EC 1.14.13.59), allowing the subsequent formation of hydrazinoacetate (Matsuda et al., 2018). The NMO-catalyzed N5-hydroxylation of ornithine is the first step in the production of piperazate (Du et al., 2017; Neumann et al., 2012), an important non-proteinogenic building block for many natural products (Morgan et al., 2019).

The pharmacologically-relevant ethionamide monooxygenase from *Mycobacterium tuberculosis* (EtaA) represents a BVMO-like FPMO (Fraaije et al., 2004). According to phylogenetic analyses, it situates between subgroups B1 and B2 (Riebel et al., 2013). EtaA activates the prodrug ethionamide by selective oxygenation and thus allows to treat *Mycobacterium* infections. *Acinetobacter radioresistens* contains a BVMO (Ar-BVMO) with identical amino acid sequence as EtaA (Minerdi et al., 2016). Ar-BVMO is capable of oxidizing the anticancer drugs metabolized by human FMO3, danusertib and tozasertib, but also can oxidize other synthetic drugs, such as imipenem.

3.3. Group C

In contrast to group A and B enzymes, group C FPMOs lack the ability to reduce their FMN cofactor independently. They rely on a separate reductase to deliver reduced FMN forming a so-called two-component system. The monooxygenase component has a characteristic $(\beta/\alpha)_8$ TIM-barrel fold (Fig. 2). Among the nineteen characterized members of group C, a wide variety of oxygenation reactions are found (Fig. 3, Fig. 6).

Bacterial luciferase (LUX; EC 1.14.14.3) represents the prototype of the group C subfamily. It is the only FPMO that produces light (Fig. 6a)

(Hastings and Nealson, 1978). This feature can be applied in prokaryotic and eukaryotic reporter gene systems for the detection of a wide range of specific analytes (Phonbuppha et al., 2020; Tinikul and Chaiyen, 2016).

The crystal structure of LUX from *Vibrio harveyi* was solved in 1995 (Fisher et al., 1995; Fisher et al., 1996), but its mechanism of action is not yet fully clear (Tinikul and Chaiyen, 2016). After FMNH⁻ binding, the flavin C4a-peroxide anion is formed by the reaction with O₂ followed by the binding of the long-chain aldehyde substrate (Fig. 6, top). Recent studies with recombinant LUX from *Vibrio campbellii* showed that His45 is important for the tight binding of FMNH⁻ and that the reaction of

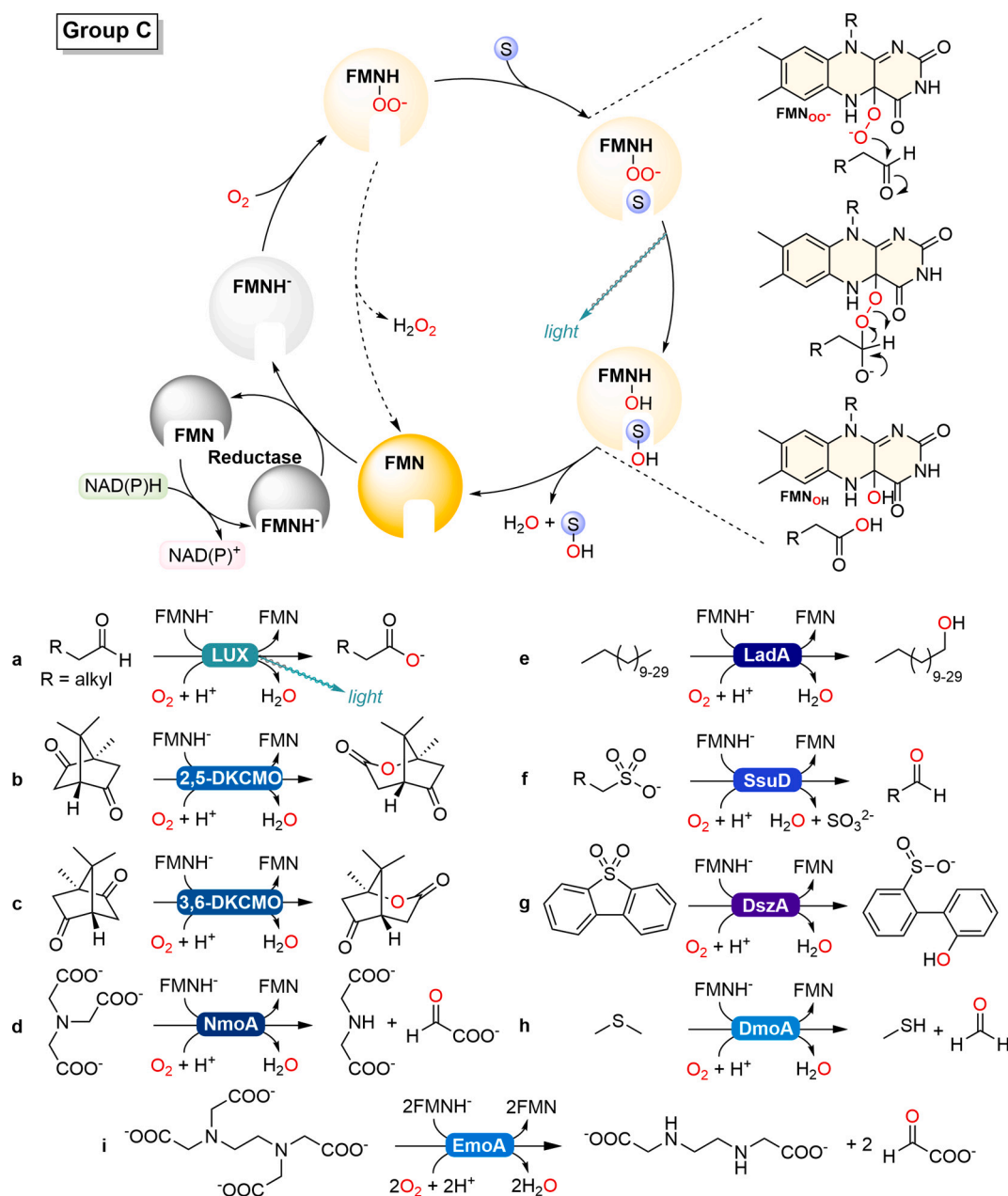


Fig. 6. Catalytic cycle of group C FPMOs. Top: The oxygenation reaction proposed for bacterial luciferase LUX from *Vibrio harveyi* is depicted, coupled to a flavin reductase component such as LuxG (Nijvipakul et al., 2008; Tinikul et al., 2013). Bottom: Overview of the substrate scope of group C enzymes. a) Baeyer-Villiger oxidation of aliphatic aldehydes to carboxylic acids with light emission by LUX; b) Baeyer-Villiger oxidation of (1R)-bornane-2,5-dione to (-)-5-oxo-1,2-campholide by 2,5-DKCMO from *Pseudomonas putida* ATCC 17453; c) Baeyer-Villiger oxidation of (1S)-bornane-2,5-dione to (+)-5-oxo-1,2-campholide by 3,6-DKCMO from *Pseudomonas putida* ATCC 17453; d) Oxidative decarboxymethylation of nitrilotriacetate to iminodiacetate and glyoxalate by NmoA from *Aminobacter aminovorans*; e) Terminal alkane oxidation of aliphatic alkanes to alcohols by LadA from *Geobacillus thermodenitrificans* NG80-2; f) Oxidative desulfonation of alkane sulfonate to aldehyde by SsuD from *Escherichia coli*; g) Oxidative ring cleavage of dibenzothiophene to 2'-hydroxybiphenyl-2-sulfinate by DszA from *Rhodococcus erythropolis* D-1; h) Oxidative dealkylation of dimethylsulfide to methanethiol and formaldehyde by DmoA from *Hyphomicrobium sulfivorans*; i) Sequential oxidative decarboxymethylation of EDTA to ethylenediaminediacetate and glyoxalate by EmoA from *Chelativorans multitrophicus*.

protein-bound FMNH⁻ with O₂ involves the initial formation of the flavin C4a-hydroperoxide (Tinikul et al., 2021). Furthermore, His44 appeared to be responsible for proton abstraction of this intermediate yielding the anionic flavin C4a-peroxide. In a Baeyer-Villiger-like reaction, the flavin C4a-peroxide nucleophile then attacks the carboxy group of the aldehyde substrate forming a Criegee intermediate-like peroxyhemiacetal state of cofactor bound substrate. Decay of this intermediate state results in the carboxylic acid product and an excited state of the C4a-hydroxyflavin, which emits light ($\lambda_{\text{max}} \approx 490$ nm) to reach the ground state. Finally, the carboxylic acid product is released, and the oxidized cofactor is recycled by the liberation of water. Kinetic studies suggested that transfer of FMNH⁻ between luciferase and its natural reductase partner occurs through free diffusion (Tinikul et al., 2013). In contrast, it has been proposed that protein-protein interaction takes place between alkanesulfonate monooxygenase from *E. coli* (SsuD; EC 1.14.14.5) and flavin reductase SsuE, leading to a more efficient channeling of FMNH⁻ between the two enzymes (Ellis, 2010).

In terms of applications, group C enzymes perform important reactions like alkane oxygenations and regioselective Baeyer-Villiger oxidations. Long-chain alkane monooxygenase from thermophilic *Geobacillus* species (LadA; EC 1.14.14.28) is of special interest, catalyzing the hydroxylation of extremely long-chain alkanes (C12 to C32) to the corresponding primary alcohols (Fig. 6e) (Boonmak et al., 2014). These building blocks are essential industrial precursors for many products, whereas in nature, *Geobacilli* and related species play an important role in crude oil degradation. Random mutagenesis of LadA from *Geobacillus thermodenitrificans* was applied to improve catalysis (Dong et al., 2012). Structural analysis revealed that most beneficial mutations appeared to be connected to residues located outside the active site, which complicates targeted mutagenesis.

Other biotechnologically relevant group C enzymes are the 2,5-diketocamphane 1,2-monooxygenase (2,5-DKCMO; EC 1.14.14.108) and the enantiocomplementary 3,6-diketocamphane 1,6-monooxygenase (3,6-DKCMO; EC 1.14.14.155 (Jones et al., 1993)) (Fig. 6b and 6c) (Isupov et al., 2015; McGhie et al., 1998), which are involved in the degradation of camphor in *Pseudomonas putida* ATCC 17453 (Bradshaw et al., 1959; Willetts, 2019). DKCMOs are generally referred to as type II BVMOs (Riebel et al., 2014; Willetts, 1997), which catalyze different regio- and enantiospecific oxidations of cyclic and aliphatic ketones, thereby generating chiral lactone products of value as synthons in chemoenzymatic synthesis (Bradshaw et al., 1959; Willetts, 2019). For example, 2,5-DKCMO catalyzes the Baeyer-Villiger oxidation of (1R)-bornane-2,5-dione (2,5-diketocamphane) to (-)-5-oxo-1,2-campholide (Fig. 6b). This chiral ketolactone spontaneously hydrolyzes to (1R)-2,2,3-trimethyl-5-oxocyclopent-3-enyl acetate. These enzymes also catalyze the oxidation of sulfide compounds to their corresponding chiral sulfoxides, albeit with an average moderate enantiomeric excess (Beecher and Willetts, 1998).

Although the 2,5-DKCMO was discovered 60 years ago (Table 1) (Bradshaw et al., 1959; Conrad et al., 1961), it took over 30 years to obtain a highly pure enzyme preparation (Table 1) (Jones et al., 1993; McGhie and Littlechild, 1996; Taylor and Trudgill, 1986). More recent transcription studies indicate that the challenge in attaining pure enzyme was related to the induction characteristics of DKCMO isoforms (Willetts et al., 2018). Two 2,5-DKCMO isoforms and a single 3,6-DKCMO from *P. putida* have now been produced via recombinant expression in *E. coli* (Iwaki et al., 2013; Kadow et al., 2012) and a crystal structure of recombinant 3,6-DKCMO is available (Table 1) (Isupov et al., 2015; McGhie et al., 1998).

Several group C enzymes catalyze the oxidative cleavage of carbon-sulfur bonds. These FPMOs can be found especially in soil bacteria which degrade organic sulfur compounds for acquisition of sulfur or for bioremediation purposes. Dimethylsulfide monooxygenase (DmoA; EC 1.14.13.131; Fig. 6h) (Cao et al., 2018)) dimethylsulfone monooxygenase (SfnG; EC 1.14.14.35 (Wicht, 2016)), and methanesulfonate monooxygenase (MsuD; EC 1.14.14.34 (Kertesz et al., 1999)) catalyze

specific oxidative demethylation steps during sulfur assimilation in bacteria. From an industrial perspective, these enzymes could be useful in waste treatment. The already mentioned SsuD catalyzes an oxidative desulfonation/dealkylation reaction giving access to C1 to C14 aldehydes (Fig. 6f) (Robbins and Ellis, 2019). Dibenzothiophene sulfone monooxygenase (DszA; 1.14.14.22 (Adak and Begley, 2016; Gray et al., 1996)) catalyzes an oxidative ring-opening reaction caused by the carbon-sulfur bond cleavage (Fig. 6g) (Adak and Begley, 2016, 2017a). Recently, this reaction was proposed to initially involve the formation of a covalent adduct between the anionic flavin N5-peroxide and the substrate and that, after subsequent splitting of the carbon-sulfur bond, the oxygen-oxygen bond of the flavin-substrate adduct is cleaved, affording the monooxygenated product 2-(2-hydroxyphenyl)-benzene sulfonate and flavin N5-oxide (Matthews et al., 2020).

Equally relevant for waste and water treatment are nitrilotriacetate monooxygenase (NmoA; EC 1.14.14.10; Fig. 6d) (Xu et al., 1997; Xun et al., 1996)) and ethylenediaminetetraacetate (EDTA) monooxygenase (EmoA; EC 1.14.14.33; Fig. 6i) (Jun et al., 2016; Payne et al., 1998; Witschel et al., 1997). These enzymes catalyze oxidative decarboxymethylation reactions, thereby assisting in the microbial degradation of the extensively used chelating agents. EmoA sequentially removes two carboxymethyl groups from EDTA and has a broader substrate range than NmoA. EmoA and NmoA use an extended lid for sealing off the substrate binding site (Jun et al., 2016). This lid is more prominent than in LadA, SsuD and bacterial luciferase. The EmoA dimer was shown to physically interact with its tetrameric partner reductase EmoB, pointing again to coupled channeling of FMNH⁻ (Jun et al., 2016).

3.4. Group D

For group D, more than 40 different FPMOs are described which have an acyl-CoA dehydrogenase fold in common and act together with a respective flavin reductase as a two-component system (Fig. 7). Group D enzymes are further divided phylogenetically in one FAD- and one FMN-dependent clade making it the only group with dual cofactor preference. Despite this, catalyzed reactions do not depend on the clade and span from hydroxylation reactions and oxidative *ipso*-substitutions of aromatic rings to heteroatom oxidation. In the natural environment, many group D members are involved in the microbial degradation of (halo) phenols (Chenprakhon et al., 2019; Pimviriyakul et al., 2017).

The general mechanism of Group D enzymes is the electrophilic attack of the reactive flavin C4a-hydroxyperoxide on the substrate resulting in hydroxylation of aromatic rings or heteroatoms. The prototype aromatic hydroxylase of group D, 4-hydroxyphenylacetate 3-hydroxylase from *Acinetobacter baumannii* (C2-HpaH; EC 1.14.14.9; Fig. 7a), has been studied in great detail (Chenprakhon et al., 2020; Pitsawong et al., 2020). Although the oxygenation reaction is similar to those catalyzed by group A enzymes, the mechanism differs since group D enzymes are two-component systems (Fig. 7, top). C2-HpaH accepts reduced FMN from the C1-HpaH reductase before molecular oxygen reacts with the cofactor to form the flavin C4a-hydroxyperoxide intermediate. Substrate binding triggers a conformational change accelerating the electrophilic reaction of the peroxide species with 4-hydroxyphenylacetate. The catalytic cycle is completed by the release of the product and water elimination from the FMN cofactor. A specific feature of the *Acinetobacter baumannii* FPMO system is that the large C1-HpaH reductase contains a regulatory site for 4-hydroxyphenylacetate binding, which is required for flavin reduction. This differs from FAD-dependent two-component HPAH systems which employ much smaller flavin reductases (Chenprakhon et al., 2020). C2-HpaH has been engineered for biocatalytic applications. Using site-directed mutagenesis, it was possible to create enzyme variants that hydroxylate alternative substrates like 4-hydroxycinnamate, 4-aminophenylacetate, tyramine and octapamine yielding valuable antioxidants and catecholamine synthons (Chenprakhon et al., 2020).

Another interesting mechanistic aspect for group D enzymes is their

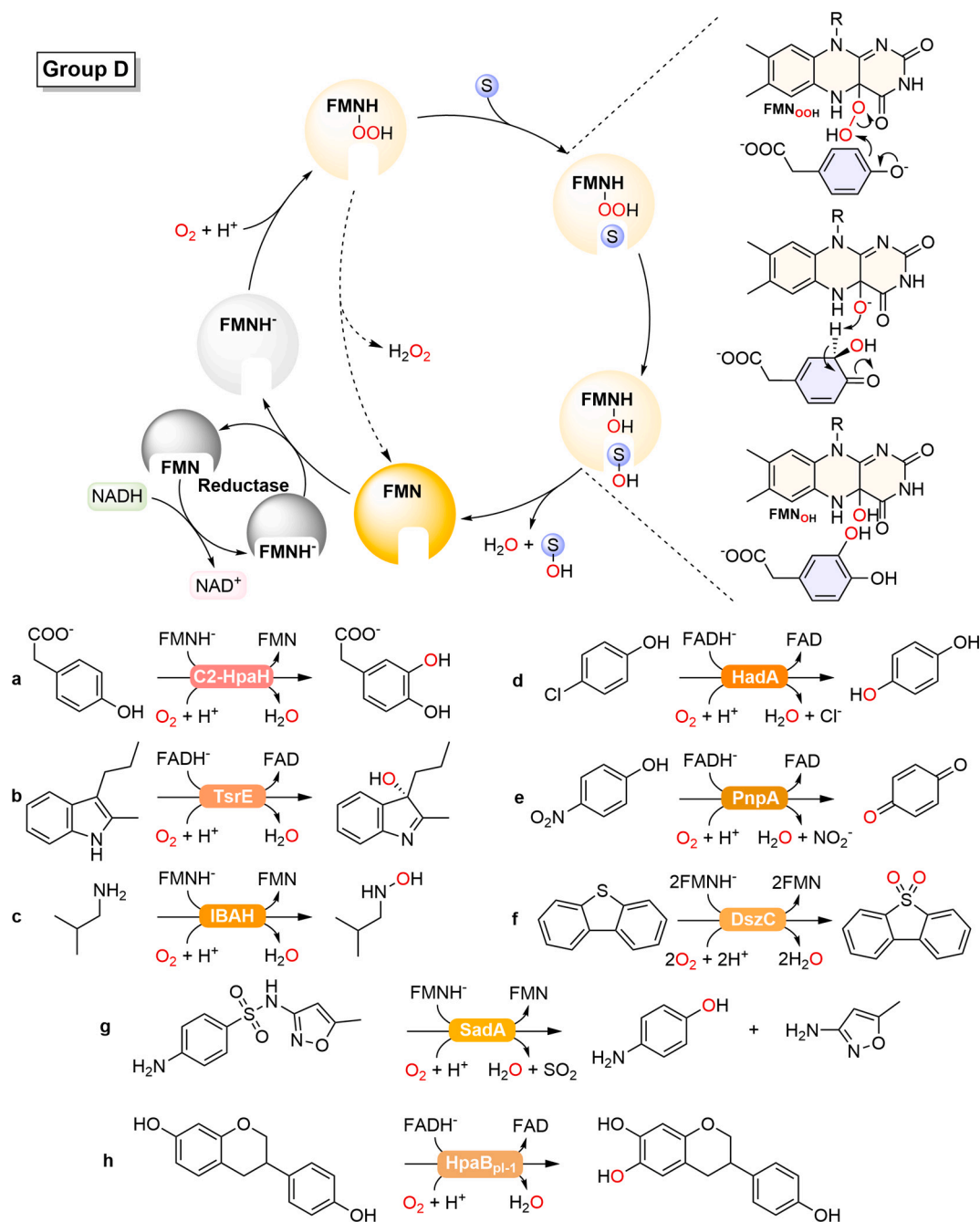


Fig. 7. Catalytic cycle of group D FPMOs. Top: The oxygenation reaction proposed for C2-HpaH from *Acinetobacter baumannii* is depicted. Bottom: Overview of the substrate scope of group D enzymes. a) Hydroxylation of 4-hydroxyphenylacetate to 3,4-dihydroxyphenylacetate by C2-HpaH; b) Hydroxylation of 2-methyl-3-propylindole to (*S*)-2-methyl-3-propyl-3*H*-indol-3-ol by TsrE from *Streptomyces laurentii*; c) *N*-hydroxylation of isobutylamine to *N*-isobutylhydroxylamine by IBAH from *Streptomyces viridifaciens*; d) Oxidative dehalogenation of 4-chlorophenol to hydroquinone by HadA from *Ralstonia pickettii*; e) Oxidative denitration of 4-nitrophenol to benzoquinone by PnpA from *Rhodococcus opacus*; f) Sulfoxidation of dibenzothiophene to dibenzothiophene sulfone by DszC from *Rhodococcus erythropolis*; g) Oxidative desulfonation of sulfamethoxazole to 3-amino-5-methylisoxazole and 4-aminophenol by SadA from *Microbacterium* sp. BR1; h) Hydroxylation of equol to 6-hydroxyequol by 4-hydroxyphenylacetate 3-hydroxylase HpaB_{pl-1} from *Photorhabdus luminescens*.

role as bifunctional enzymes in several metabolic pathways. It is known that *ipso*-substitutions and hydroxylation reactions can be performed sequentially because the underlying mechanism is quite similar. The same holds true for sulfoxidations for which in two oxidative steps a sulfide is transformed to a sulfone. 4-Nitrophenol 4-monooxygenase (PnpA; EC 1.14.13.167) from *Rhodococcus opacus* catalyzes the oxidative denitration of 4-nitrophenol to benzoquinone (Fig. 7e), which is then further converted to 1,2,4-trihydroxybenzene (Kitagawa et al., 2004). 4-Chlorophenol monooxygenase (HadA) from *Ralstonia pickettii* (Fig. 7d)

has been engineered to catalyze sequential oxidative dehalogenation and denitration reactions (Pimviriyakul and Chaiyen, 2018). Dibenzothiophene monooxygenase (DszC; EC 1.14.14.21 (Kamali et al., 2010)) from *Rhodococcus erythropolis* catalyzes the sequential sulfoxidation of dibenzothiophene (DBT) to DBT-sulfoxide and DBT-sulfone, respectively (Fig. 7f). In this way, the enzyme initiates the microbial desulfurization of crude oil (Guan et al., 2015).

Equol mining was used to search for monooxygenases that can convert the nutritional supplement (*S*)-equol to commercially

unavailable hydroxyequols (Hashimoto et al., 2019). It was found that one of the HpaH homologues from *Rhodococcus opacus* efficiently converts both (*R*)- and (*S*)-equols to the corresponding 3'-hydroxyequols with a slight preference for the (*S*)-enantiomer, and that one of the HpaH homologues from *Photorhabdus luminescens* (HpaB_{pl-1}) regioselectively hydroxylates the (*R*)- and (*S*)-equols to the corresponding 6-hydroxyequols (Fig. 7h) with clear preference for the (*S*)-enantiomer. 3-Hydroxy-9,10-secoandrosta-1,3,5(10)-triene-9,17-dione monooxygenase (HsaA; EC 1.14.14.12 (Dresen et al., 2010)), involved in the catabolism of cholesterol in *Mycobacterium tuberculosis*, is a group D member that is active with a steroid substrate.

Another interesting reaction catalyzed by a group D member concerns the oxidative desulfonation of the widely used antibiotic sulfamethoxazole. This reaction is catalyzed by sulfonamide monooxygenase (SadA), which initiates the catabolism of various sulfonamides in *Microbacterium* species through an *ipso*-hydroxylation mechanism (Fig. 7g) (Ricken et al., 2017). In the next step, another FMN-dependent group D member, 4-aminophenol monooxygenase (SadB), converts the released 4-aminophenol by sequential oxidative deamination and hydroxylation to the ring-cleavage substrate 1,2,4-trihydroxybenzene (Ricken et al., 2017).

Several group D enzymes catalyze indole oxidations, such as 2-methyl-indolylpyruvate 3-hydroxylase (TsrE) from *Streptomyces laurentii*. This enzyme, which initiates an unusual indole-ring expansion mechanism in the biosynthesis of thiostrepton, was found to hydroxylate the synthetic substrate mimic 2-methyl-3-propylindole (Fig. 7b), triggering a double bond shift within the pyrrole ring, yielding the (3*S*)-isomer of the imine product with an enantiomeric excess (*ee*) value up to 96% (Lin et al., 2017).

Indole 3-acetate monooxygenase (IacA; EC 1.14.13.235) catalyzes the initial step in the degradation of the plant hormone auxin in *Pseudomonas putida* yielding 2-hydroxy-indole-3-acetate as most likely product (Scott et al., 2013). IacA is also capable of oxidizing indole to indoxyl, which spontaneously dimerizes to the blue pigment indigo. Recently, a IacA homologue from *Caballeronia glathei* DSM50014 was described to accept a variety of indole derivatives (Sadauskas et al., 2020). In this study, the initial activation of indole 3-acetate was proposed to occur via epoxidation as recently demonstrated for group E monooxygenases (Heine et al., 2019). Indosespene 3-hydroxylase (XiaF) catalyzes the conversion of indosespene to the carbazole moiety of the indolosesquiterpenoid xiamycin in *Streptomyces* endophytes (Kugel et al., 2017). This cryptic cyclization reaction is believed to involve the initial 3-hydroxylation of the indole moiety of indosespene. XiaF also oxygenates indole to indoxyl, which spontaneously oxidizes to indigo and indirubin.

Group D enzymes also catalyze *N*-hydroxylations. One example is isobutylamine N1-monooxygenase (IBAH; EC 1.14.14.30) from *Streptomyces viridifaciens*, which catalyzes the oxidation of isobutylamine to *N*-isobutylhydroxylamine (Fig. 7c), a key step in the biosynthesis of the azoxy antibiotic valanimycin (Parry and Li, 1997). Other *N*-hydroxylations are catalyzed by dTDP-L-evernosamine *N*-hydroxylase (RubN8; EC 1.14.13.187) from *Micromonospora carbonacea* (Vey et al., 2010), dTDP-L-epivancosamine *N*-hydroxylase (DnmZ) from *Streptomyces peucetius* (Sartor et al., 2015), and dTDP-3-amino-2,3,6-trideoxy-4-keto-3-methyl-D-glucose *N*-hydroxylase (KijD3) from *Actinomadura kijaniata* (Bruender et al., 2010). The first two enzymes mediate the double oxidation of their dinucleotide aminosugar substrates to the corresponding nitrososugars, whereas KijD3 produces a nitrosugar (Thoden et al., 2013).

3.5. Group E

Group E FPMOs are flavin reductase-dependent monooxygenases containing a similar FAD-binding domain as group A enzymes. The flavin reductase fuels the independent monooxygenase with reduced FAD. Some group E FPMOs are natural fusion proteins of oxygenase and

reductase, resulting in a self-sufficient enzyme (Tischler et al., 2009; Tischler et al., 2020; Tischler et al., 2018). Based on altered substrate specificity caused by distinct active site sequence motifs, group E is divided in two subgroups (Heine et al., 2020). Subgroup E1 accommodates styrene monooxygenase (SMO; EC 1.14.14.11) with a substrate preference for styrene derivatives, whereas subgroup E2 contains indole monooxygenases (IMO) showing the highest activity with indole derivatives.

Group E enzymes catalyze enantioselective epoxidations and sulfoxidations with a general preference for (*S*)-epoxides while SMOs and IMOs have different preferences for sulfoxidations (Fig. 8; (Heine et al., 2020)). In natural environment, group E enzymes act as initial enzymes of aromatic compound detoxification, funneling the xenobiotics in aromatic degradation pathways (Tischler et al., 2020).

Mechanistically, group E enzymes perform an electrophilic attack of the flavin C4a-hydroxyperoxide intermediate (Fig. 8, top). Either the carbon double bond in epoxidation reactions or the free electron pair of the sulfur atom in heteroatom oxidations acts as the respective nucleophile. Reduced FAD is delivered by the respective reductase and taken up by the oxygenase in a similar manner as described for group D enzymes. The substrate binds after formation of the flavin oxygenation species. After decomposition of the highly fluorescent flavin C4a-hydroxide (Tischler et al., 2013), the product and oxidized cofactor are released. Although the oxygenase-reductase interaction of SMO is described as weak, it was shown for the enzymes from *Pseudomonas* and *Rhodococcus* that the catalytic activity of the oxygenase is higher in presence of the reductase indicating that the interaction with the reductase promotes overall epoxidase activity (Morrison et al., 2013; Tischler et al., 2010). The fusion proteins mentioned before represent a special case where reductase and oxygenase interact compulsorily.

From an industrial point of view, there is a high interest in group E enzymes because epoxides and sulfoxides in enantiopure form are important precursors for chiral products (Di Gennaro et al., 1999; Panke et al., 2000). Recently, a highly active group E enzyme (AbIMO) was employed to produce (*S*)-2-chloro-4-(methylsulfinylmethyl)pyridine (Fig. 8d), which represents a precursor for bioactive synthetic approaches (Willrodt et al., 2020). To the best of our knowledge this system represents the highest oxygenation rate of two-component FPMOs in applied biocatalysis. In addition, group E enzymes convert many substituted aromatic and aliphatic alkenes, but also oxidize aromatic sulfides, sulfanes and benzothiophenes (Toda et al., 2012; Toda et al., 2015; Wu et al., 2017b). Next to their broad substrate scope, group E enzymes can be fueled by nicotinamide biomimetics (NBCs) making them independent of NADH supply and the corresponding reductase (Paul et al., 2015). Furthermore, group E enzymes can be optimized to withstand organic co-solvents, which can increase the substrate availability of apolar substances (Eggerichs et al., 2020). Corroborating their potential as biocatalyst, Witholt and co-workers achieved to produce gram-scale amounts of (*S*)-styrene oxide and related chiral oxiranes in a two-liquid phase fed-batch bioreactor (Panke et al., 2002; Schmid et al., 2001) (Table 1).

SMOs usually produce (*S*)-epoxides and (*R*)-sulfoxides (Fig. 8). IMOs, on the other hand, prefer (*S*)-sulfoxidations but share the preference for epoxides. Several mutagenesis studies were applied to change the enantioselectivity towards (*R*)-epoxides, but the lack of structural information has limited these approaches so far. The only known 3D-structures of group E enzymes belong to the monooxygenase and reductase component of the SMO from *Pseudomonas putida* S12 (Fig. 2) (Morrison et al., 2013; Ukaegbu et al., 2010). Although the oxygenase structure lacks substrate and cofactor positions, variants with altered substrate preferences were successfully generated in a semi-rational process. The SMO Y73V variant of *Pseudomonas putida* S12 converts 1-phenylcyclohexene into the (*R,R*)-epoxide instead of the normally produced (*S,S*)-enantiomer. Amino acid residues relevant for substrate recognition and selective oxygenation were recently described for 31 group E monooxygenases (Heine et al., 2020). Therein, two fingerprint motives (SMO

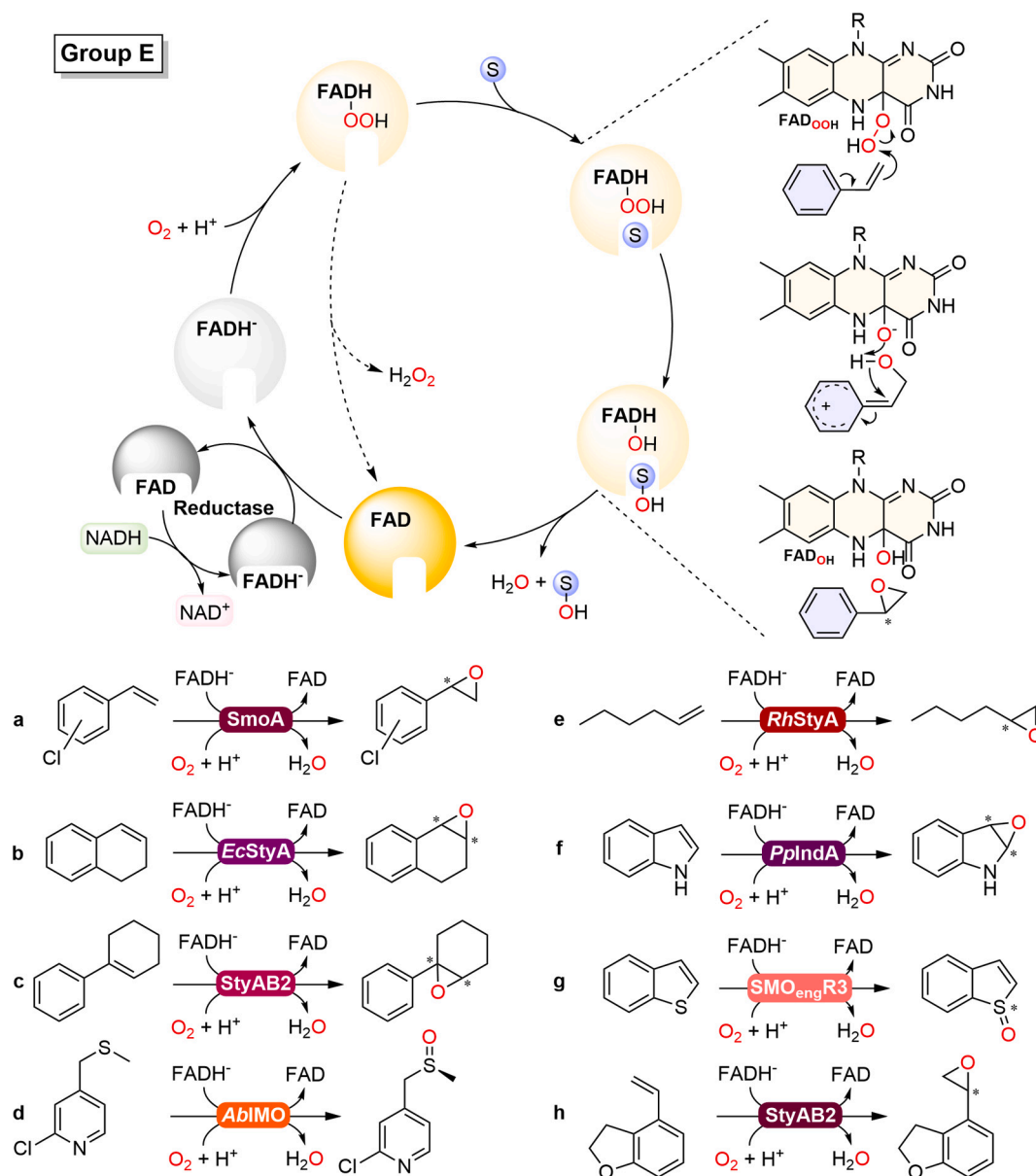


Fig. 8. Catalytic cycle of group E FPMOs. Top: The oxygenation reaction proposed for StyA is depicted. Bottom: Overview of the substrate scope of group E enzymes. a) Epoxidation of chlorostyrenes to chlorostyrene oxides by styrene monooxygenase SmoA found in environmental metagenome; b) Epoxidation of 1,2-dihydronaphthalene to 1,2-dihydronaphthalene oxide by styrene monooxygenase EcStyA from *Escherichia coli*; c) Epoxidation of 1-phenyl-1-cyclohexene to its corresponding oxide by fusion styrene monooxygenase StyAB2 from *Pseudomonas* sp. LQ26; d) Sulfoxidation of 2-chloro-4-(methylsulfanylmethyl)pyridine to (S)-2-chloro-4-(methylsulfinylmethyl)pyridine by indole monooxygenase AbIMO from *Acinetobacter baylyi* ADP1; e) Epoxidation of 1-hexene to 1,2-epoxyhexane by styrene monooxygenase RhStyA from *Rhodococcus* sp. ST-10; f) Epoxidation of indole to its epoxy indole by indole monooxygenase PpIndA from *Pseudomonas putida*; g) Sulfoxidation of 1-benzothiophene to 1-benzothiophene-1-oxide by engineered styrene monooxygenase SMO_{eng}R3 from *Pseudomonas putida* CA-3; h) Epoxidation of 4-vinyl-2,3-dihydrobenzofuran to 4-(oxiran-2-yl)-2,3-dihydrobenzofuran by StyAB2 from *Pseudomonas* sp. LQ26.

N46-V48-H50-Y73-H76-S96 and IMO S46-Q48-M50-V/I73-I76-A96) were identified which allow distinguishing SMO and IMO enzymes as well as provide hints towards enantio-preference in epoxidation (degree of purity among *S*-epoxides) as well as sulfoxidation (selectivity for *S*- or *R*-sulfoxide) reactions. In addition to the ongoing mutagenesis optimization, Wu and co-workers identified recently a SMO from the genome of *Streptomyces* sp. NRRL S-31 that showed complementary stereoselectivity toward alkenes and only formed the (*R*)-epoxides (Cui et al., 2020).

Heine and co-workers designed artificial fusions of StyA and StyB from *Pseudomonas fluorescens* ST to produce Tyrian purple and other indigoid dyes (Heine et al., 2019; Heine et al., 2017). Similarly, the group of Mutti used a flexible linker between StyA and StyB from

Pseudomonas taiwanensis VLB120, and co-expressed this self-sufficient SMO with a formate dehydrogenase to improve the efficiency of (*S*)-styrene oxides production (Corrado et al., 2018). This chimeric SMO was integrated in a multienzyme cascade (Wu et al., 2017a) for the regio- and stereoselective aminohydroxylation of *trans*- β -methylstyrene affording enantiopure (1*R*,2*R*)- and (1*S*,1*R*)-phenylpropanolamine diastereomers (Corrado et al., 2019).

3.6. Group F

Group F enzymes are structurally related to group A enzymes and share the characteristic FAD-binding scaffold of the glutathione reductase superfamily (GR-2). The 40 described group F enzymes can be

differentiated from group A by a specific WxWxIP active-site sequence motif called W-box fingerprint (Zhu et al., 2009). FPMOs of group F comprise two-component FAD-dependent halogenases (FDHs) that typically catalyze bromination or chlorination steps during the biosynthesis of natural products (Fig. 9) (Agarwal et al., 2017; Gkotsi et al., 2018; Latham et al., 2018; van Pée et al., 2006). Most FDHs catalyze halogenations of free indoles (Fig. 9d), pyrroles and phenols, while others are active with carrier protein bound substrates in non-ribosomal peptide synthetase or polyketide synthase assembly lines (Agarwal et al.,

2017; Latham et al., 2018).

The first FDH obtained in pure form was tryptophan 7-halogenase from *Pseudomonas fluorescens* (PrnA; EC 1.14.19.9 (Keller et al., 2000)). The elucidation of its crystal structure was a real breakthrough (Table 1) (Dong et al., 2005). The PrnA structure supported the view that flavin C4a-hydroxyperoxide performs an electrophilic attack on a chloride anion forming the respective hypochlorous acid (HOCl) (Fig. 9, top), which is channeled to the substrate binding site (Dong et al., 2005). Here, HOCl is activated by a lysine residue stimulating the regioselective

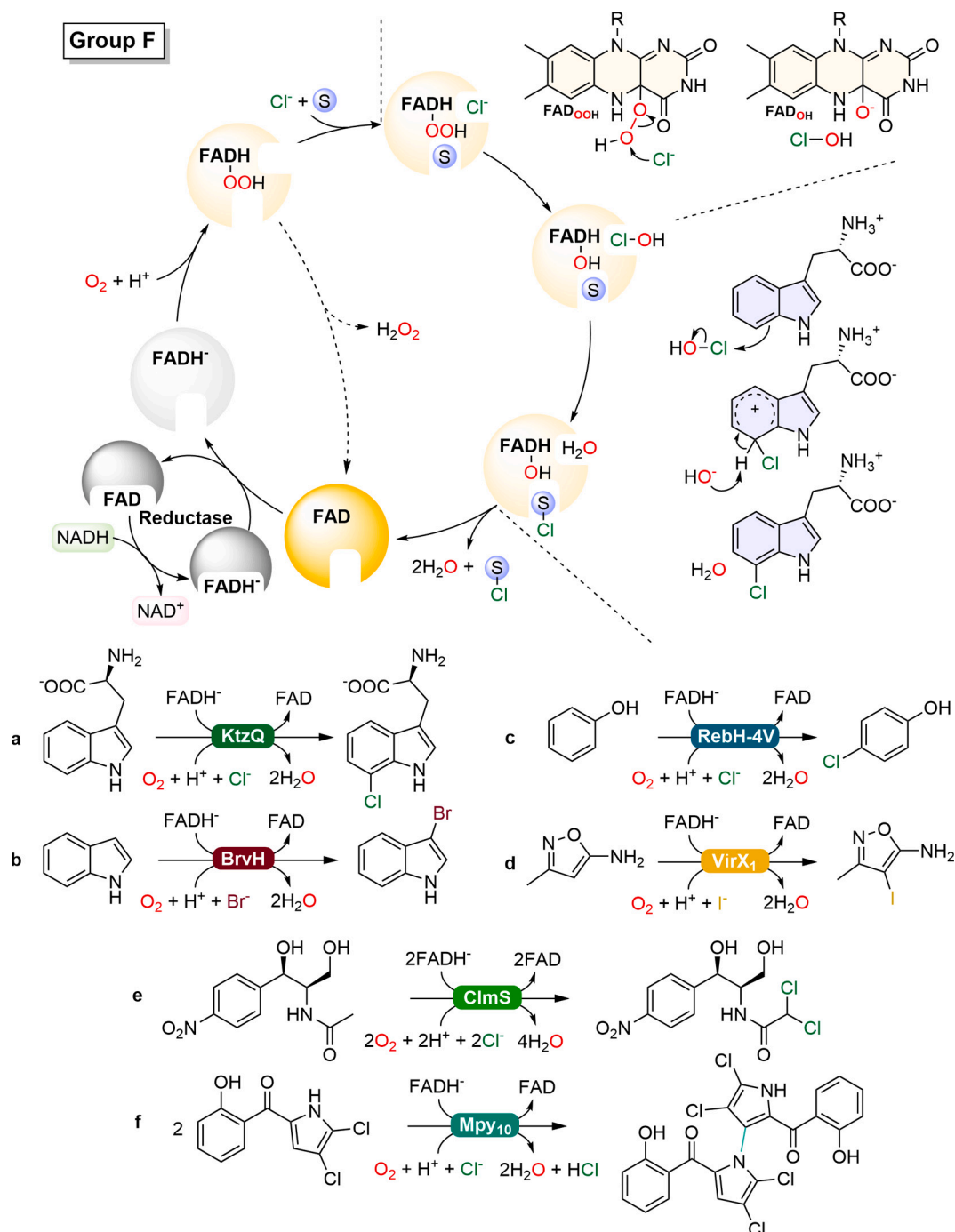


Fig. 9. Catalytic cycle of group F FPMOs. Top: The oxygenation reaction proposed for tryptophan 7-halogenase KtzQ from *Kutzneria* sp. 744 is depicted. Bottom: Overview of the substrate scope of group F enzymes. a) Chlorination of L-tryptophan to 7-chloro-L-tryptophan by KtzQ; b) Bromination of indole to 3-bromoindole by the FDH BrvH found in maritime bacterial metagenome; c) Chlorination of phenol to 4-chlorophenol by FDH mutant RebH-4V from *Lechevalieria aerocolonigenes*; d) Iodination of 3-methylisoxazol-5-amine to 4-iodo-3-methylisoxazol-5-amine by the FDH VirX1 from cyanophage metagenome; e) Alkane halogenation of N-acetyl-p-nitrophenylserinol to chloramphenicol by FDH ClmS from *Streptomyces venezuelae*; f) C,N-biaryl coupling of deoxyppyolutorin to a marinopyrrole dimer by FDH Mpy10 from *Streptomyces* sp. CNQ-418.

attack on tryptophan. Following the mechanism of an electrophilic aromatic substitution, the positive charge of the intermediate state is stabilized by delocalization before a proton is abstracted and aromaticity is restored (Fig. 9, top). Subsequent mutagenesis and crystallography studies on tryptophan 7-halogenases PrnA and RebH (Bitto et al., 2008; Yeh et al., 2005), tryptophan 5-halogenase PyrH (EC 1.14.19.58 (Zhu et al., 2009)), and Trp 6-halogenases Thal and BorH (EC 1.14.19.59), confirmed the catalytic role of the conserved lysine and showed slightly different binding modes of tryptophan explaining the regioselectivity of halogenation (Schnepel and Sewald, 2017).

For halogenations of activated aliphatic substrates like the antibiotic chloramphenicol, an acid-catalysis at the carbonyl oxygen can be assumed to lower the pK_a value of the C_α protons. This allows the tautomerization to the enol form which similarly performs an electrophilic attack on the hypohalogenous acid. The most favored halogen utilized is chlorine, although many FDHs also accept bromine, albeit with decreased activity. Nevertheless, a few enzymes have been discovered, which prefer bromine over chloride or are even active with iodine (Gkotsi et al., 2019; Neubauer et al., 2018).

FDHs are of interest for the production of antibiotics, antitumor agents and other natural products which require regioselective halogenation under mild and green conditions (Frese and Sewald, 2015). Furthermore, the natural flavin reductase redox partner can be replaced for biocatalytic reactions *in vitro* by (photo)chemically reduced FAD, allowing a more cost-efficient process (Ismail et al., 2019; Schroeder et al., 2018; Unversucht et al., 2005).

KtzR (EC 1.14.19.60) is a tryptophan halogenase involved in the assembly of the antifungal secondary metabolite kutzneride, and selectively converts 7-chlorotryptophan, originally produced by KtzQ (Fig. 9a), to 6,7-dichlorotryptophan (Heemstra and Walsh, 2008). Another unusual tryptophan halogenase, obtained from the marine sponge *Theonella swinhoei* WA, catalyzes the 6-chlorination of 5-hydroxytryptophan, also being quite active with serotonin and 5-methoxyindole (Smith et al., 2017).

Next to engineering the regioselectivity of halogenation and the discovery of novel family members, efforts have been spent towards increasing the catalytic efficiency, broadening the substrate scope, and improving the thermal- and operational stability of FDHs (Andorfer and Lewis, 2018; Latham et al., 2018). Employing genome mining with a previously unappreciated sequence motif, Goss and co-workers discovered the first FDH (VirX1) that exhibits a clear preference for iodination (Fig. 9d) and acts on a diverse set of organic substrates (Gkotsi et al., 2019).

FDHs are also capable of catalyzing sequential halogenations. The first example of such reaction was reported for PltA from *Pseudomonas fluorescens*, which catalyzes the dichlorination of pyrrolyl-S-PltL during the biosynthesis of the antifungal natural product pyoluteorin (Dorrestein et al., 2005). Another example is represented by MaLA and MaLA' from *Malbranchea aurantiaca*. Both FDH isoforms catalyze the chlorination and bromination of premalbrancheamides during late-stage fungal alkaloid biosynthesis (Fraley et al., 2017). ClmS from *Streptomyces venezuelae* is one of the few FDHs known that halogenates an activated alkyl substrate, forming the dichloroacetyl group of chloramphenicol (Fig. 9e) (Podzelinska et al., 2010).

A pair of FDHs (Mpy10 (Fig. 9f), and Mpy11) from *Streptomyces* sp. CNQ-418 was shown to catalyze the chiral N,C-biaryl coupling of two molecules of monodeoxytryptoliteorin (Hughes et al., 2010), which results in densely halogenated marinopyrroles possessing potent antibiotic activity (Yamanaka et al., 2012). This discovery adds an interesting reaction type to the profile of group F enzymes.

Recently, Lewis and co-workers employed family-wide activity profiling to obtain sequence-function information on FDHs (Fisher et al., 2019). Using a high-throughput mass-spectrometry-based screen of more than 100 putative FDH sequences they identified halogenases with novel substrate scope and complementary regioselectivity and used these enzymes for preparative scale C-H functionalization. The Lewis

group also reported engineered FDHs that catalyze the bromolactonisation of olefins with high enantioselectivity (Mondal et al., 2020). This oxidative halocyclization reaction broadens the catalytic repertoire of FPMOs (Fig. 3).

3.7. Group G

Group G enzymes are single-component FAD-dependent mono-oxygenases containing a monoamine oxidase fold (Fig. 2). They are classified as self-sufficient or internal monooxygenases, reducing their flavin cofactor via substrate oxidation and thus circumventing the requirement of a reductase and stoichiometric consumption of NAD(P)H. Group G enzymes hardly stabilize the flavin C4a-hydroperoxide. They have been proposed to use enzyme-bound hydrogen peroxide for the monooxygenation of the intermediate product, generated during the reductive half-reaction (Fig. 10) (Lockridge et al., 1972; Ralph et al., 2006).

Group G enzymes catalyze oxygenative decarboxylation reactions of several amino acids such as arginine (AMO; EC 1.13.12.1 (van Thoai and Olomucki, 1962a, 1962b)), lysine (LMO; EC 1.13.12.2; Fig. 10a) (Ohnishi et al., 1976)), tryptophan (TMO; EC 1.13.12.3 (Gaweska et al., 2013)) and phenylalanine (PAO; EC 1.13.12.9; Fig. 10b) (Ida et al., 2008)) to give the corresponding amides. Depending on the amino acid used, group G enzymes can also function as oxidases, thereby converting the intermediate imino acids through oxidative deamination to α -keto acids (Fig. 10a and 10b).

The two-step mechanism of group G enzymes is initiated by the oxidation of the amino acid substrate resulting in a reduction of the FAD cofactor and the formation of an imino acid (Fig. 10, top). Two alternative routes have been proposed for the oxygenation of the imino acid. In one route, C4a-hydroxyperoxy-FAD is formed by the reaction of the reduced cofactor with molecular oxygen (Fig. 10, top right). The peroxide intermediate performs an electrophilic attack on the C_α carbon atom of the imino acid eliminating carbon dioxide. The formed imidic acid tautomerizes to the amide product, and the oxidized flavin cofactor is regenerated from flavin C4a-hydroxide by cleavage of water. In the alternative route, the C4a-hydroxyperoxy-FAD is not stabilized upon reaction of the reduced flavin with oxygen, and the imino acid reacts with the formed hydrogen peroxide (Fig. 10, top middle).

Tryptophan 2-monooxygenase (TMO; EC 1.13.12.3 (Gaweska et al., 2013)) is the prototype enzyme of this group of internal monooxygenases. The enzyme catalyzes the oxygenative decarboxylation of tryptophan to yield the plant growth hormone indole-3-acetamide (Ralph et al., 2006). The catalytic mechanism of TMO has been studied in detail and the predicted role of several active site residues was confirmed after solving the 3D structure (Gaweska et al., 2013; Sobrado and Fitzpatrick, 2003a, 2003b). Decarboxylation of the imino acid to the amide is thought to occur in the TMO active site through reaction with free hydrogen peroxide.

Another group G member with known structure concerns phenylalanine 2-monooxygenase from *Pseudomonas* sp. P-501 (PAO; EC 1.13.12.9 (Ida et al., 2008)). PAO catalyzes oxygenative decarboxylation of L-phenylalanine and oxidative deamination of L-methionine. Although not detected during the oxidative half-reaction, PAO has been proposed to use the flavin C4a-hydroperoxide adduct for substrate oxygenation (Ida et al., 2011).

LMO from *Pseudomonas* sp. AIU813 catalyzes both the decarboxylation and deamination of L-lysine (Matsui et al., 2014). Based on the earlier proposal for PAO (Ida et al., 2011), oxygenation of the intermediate imino acid was assumed to involve the participation of flavin C4a-hydroperoxide (Im et al., 2018). However, studies from rapid kinetics and mass-spectrometry product analysis indicated that LMO from *Pseudomonas* sp. AIU813 does not stabilize flavin C4a-hydroperoxide, and that the *in situ* generated enzyme-bound hydrogen peroxide decarboxylates the imino lysine to 5-aminovaleramide (Trisrivirat et al., 2020). The fact that the alternative substrate L-ornithine was mainly

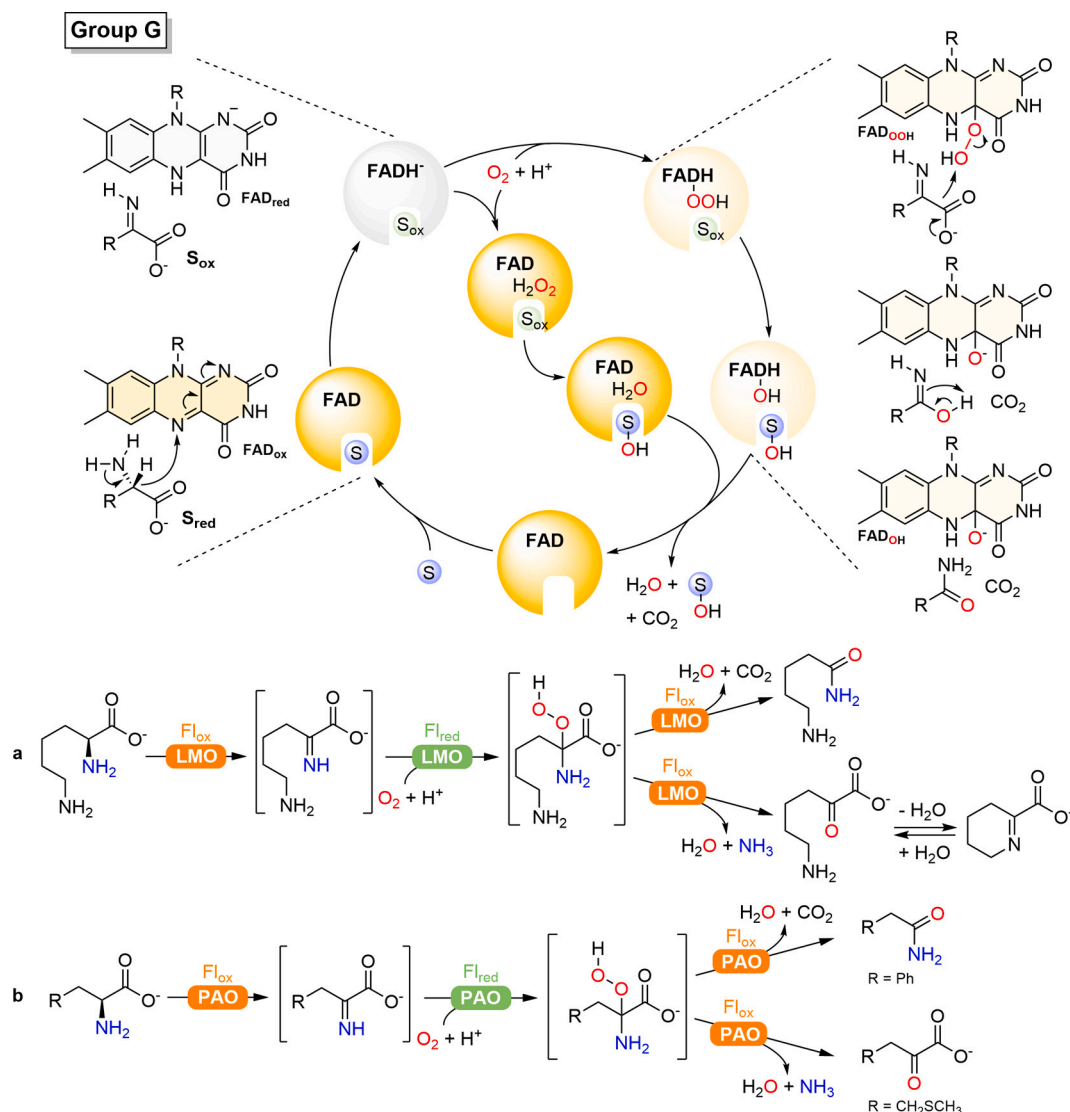


Fig. 10. Catalytic cycle of group G FPMOs. Top: Two alternative oxygenation routes proposed for LMO are depicted (see text for further explanation). Bottom: Overview of the substrate scope of group G enzymes. a) Oxidative decarboxylation of L-lysine to 5-aminopentanamide or deamination of L-lysine to 6-amino-2-oxohexanoate by lysine 2-monooxygenase LMO from *Pseudomonas fluorescens*; b) Oxidative decarboxylation of L-phenylalanine to 2-phenylacetamide or deamination of L-methionine to 4-(methylthio)-2-oxobutanoate by PAO from *Pseudomonas* sp. P-501.

converted by oxidative deamination to 2-keto-5-aminovaleric acid pointed to a critical fine-tuning of the position of bound hydrogen peroxide and imino acid in the active site of the re-oxidized enzyme (Trisrivirat et al., 2020). These results merit further investigation, not only from a mechanistic point of view, but also to see if it is possible to optimize the group G reactions for the production of interesting platform chemicals.

From a biotechnological point of view, group G enzymes are of interest as cofactor-free self-sufficient oxidases. Nevertheless, their substrate scope is limited and remains to be further explored.

3.8. Group H

Group H comprises internal FPMOs with a $(\beta/\alpha)_8$ TIM-barrel fold (Fig. 2), catalyzing oxidative decarboxylation and denitration reactions (Fig. 3). The mechanism of the oxidative decarboxylation reaction of group H enzymes resembles that of group G enzymes (cf. Fig. 10). However, the oxidative denitration reaction follows a radical mechanism, which is quite unusual for FPMOs (Fig. 3).

LaMO was the first discovered flavoprotein monooxygenase and for a

long time the only representative of group H. LaMO catalyzes the oxidation of L-lactate to acetate via the oxidative decarboxylation of the initially formed pyruvate (Fig. 11b) (Edson, 1947). LaMO from *Mycobacterium phlei* was first purified in 1954 (Table 1) (Sutton, 1954), but it took another three years to firmly establish that the enzyme contained an FMN cofactor (Sutton, 1955, 1957) and catalyzes a monooxygenation reaction (Hayaishi and Sutton, 1957). LaMO shares many properties with flavin-dependent α -hydroxyacid oxidases (Giegel et al., 1990; Maeda-Yorita et al., 1995; Stoisser et al., 2016; Sun et al., 1996), but the structural requirements for its monooxygenase activity remained for a long time unclear. In 2018, the crystal structure of LaMO from *Mycobacterium smegmatis* was elucidated (Kean and Karplus, 2019). From structural comparison with the related α -hydroxyacid oxidases, it was proposed that the stability of a large and compact active site lid in LaMO is responsible for the slow release of pyruvate from the re-oxidized enzyme, facilitating its reaction with enzyme-bound hydrogen peroxide (Kean and Karplus, 2019).

Recently, the proposed mechanism for the flavoenzyme-catalyzed oxidative decarboxylation of α -keto-acids was challenged again. The Y128F variant of the FMN-containing (*S*)-*p*-hydroxymandelate oxidase

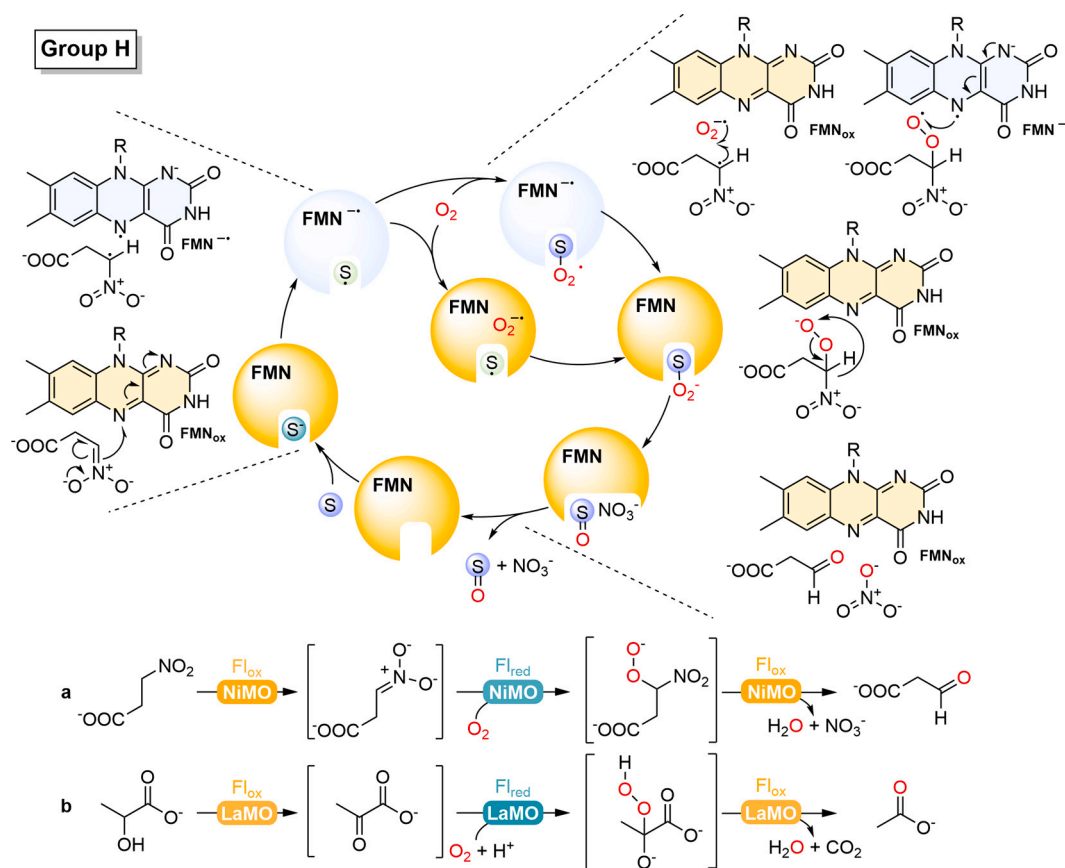


Fig. 11. Catalytic cycle of group H FPMOs. Top: Two alternative oxygenation routes proposed for NiMO from *Pseudomonas aeruginosa* are depicted. Bottom: Overview of the substrate scope of group H enzymes. a) Oxidative alkane denitration of nitronate to 3-oxopropanoate by NiMO; b) Oxidative alkane decarboxylation of lactate to acetate by LaMO from *Mycobacterium phlei*.

(Hmo; EC 1.1.3.46 (Lyu et al., 2019)), which acts as a monooxygenase (Lyu et al., 2019), was reported to form several flavin-oxygen adducts in the crystalline state when the enzyme was incubated with slow reacting substrate analogues (Lin et al., 2020). From this it was argued that the α -keto-acid intermediate products do react with flavin C4-(hydro)peroxide when this flavin oxygenation species is sufficiently stabilized. In the case of the non-decarboxylative substrate methyl (S)-mandelate, this resulted in a Baeyer-Villiger type of flavin C4a-peroxy-methyl ester adduct, whereas for the reaction with 2-hydroxy-3-oxosuccinate, initially formed from (2S,3R)-tartrate, the accumulation of a flavin C4a-N5 epoxide was proposed.

Nitronate monooxygenase (NiMO; EC 1.13.12.16 (Smitherman and Gadda, 2013)) catalyzes an oxidative denitration reaction, using molecular oxygen to oxidize the metabolic poison propionate 3-nitronate (P3N) and other alkyl nitronates to the corresponding aldehydes and nitrate (Fig. 11a). NiMOs are widespread in nature and currently more than 3000 genes are annotated to be NiMO, or alternatively to be 2-nitropropane dioxygenase, as the enzyme was officially classified until 2010 (Francis et al., 2013). Few NiMO proteins have been characterized biochemically, so that only a restricted substrate scope is known, limiting their biotechnological application (Francis et al., 2013).

The crystal structures of NiMO from *Pseudomonas aeruginosa* PAO1 (Salvi et al., 2014) and *Cyberlindnera saturnus* (Agniswamy et al., 2018) are highly conserved. NiMOs does not use a flavin C4a-oxygen adduct as oxygenating species (Gadda and Francis, 2010). Instead, spectral evidence was obtained that the enzymes from *Williopsis saturnus* readily form a substrate radical species and an anionic flavosemiquinone (Fig. 11, top) (Smitherman and Gadda, 2013). First, a carbenium ion is formed by deprotonation at the carbon atom next to the nitro group of the 3-nitropropionate substrate. Subsequent electron transfer from the

anionic flavosemiquinone to O₂ generates superoxide anion, which reacts with the substrate radical to yield 3-peroxy-3-nitropropanoate. Alternatively, the substrate radical reacts with O₂ to give a 3-peroxy-3-nitropropanoate radical, which subsequently receives an electron from the anionic flavosemiquinone. Finally, the 3-peroxy-3-nitropropanoate decays to 3-oxopropanoate, with liberation of nitrite.

4. Conclusions

FPMOs have fascinated (bio)chemists already for more than 60 years. Initially, mainly because of the intriguing way these colorful enzymes activate O₂, a molecule we depend on at every moment in life. Gradually, this fascination was shared by structural biologists and protein engineers, which led to improved understanding of the mechanistic details of the FPMO-catalyzed oxyfunctionalization reactions. The omics revolution then caused that new FPMOs were more easily discovered and produced. This boosted the knowledge about their chemo-, regio- and enantioselectivity, and stimulated their use in applied biocatalysis. As elaborated in this review, a wide range of group A to H FPMOs is available. Current efforts reveal an exponentially growing number of FPMOs, whether wild-type or variants, which can catalyze novel oxygenation chemistries and are improved for industrial application.

Author contributions

All authors contributed to the writing and figures of the review.

Acknowledgements

DE was supported by a pre-doctoral scholarship from the Deutsche

Bundesstiftung Umwelt (DBU, 20019/625) and was funded by the German Research Council (DFG) within the framework of GRK 2341 (Microbial Substrate Conversion). DT was supported by the Federal Ministry for Innovation, Science and Research of North Rhine–Westphalia (PtJ-TRI/1411ng006—ChemBioCat).

References

- Abood, A., Al-Fahad, A., Scott, A., Hosny, A.E.-D.M.S., Hashem, A.M., Fattah, A.M.A., Race, P.R., Simpson, T.J., Cox, R.J., 2015. Kinetic characterisation of the FAD-dependent monooxygenase TropB and investigation of its biotransformation potential. *RSC Adv.* 5, 49987–49995. <https://doi.org/10.1039/c5ra06693j>.
- Adak, S., Begley, T.P., 2016. Dibenzothiophene catabolism proceeds via a flavin-N5-oxide intermediate. *J. Am. Chem. Soc.* 138, 6424–6426. <https://doi.org/10.1021/jacs.6b00583>.
- Adak, S., Begley, T.P., 2017a. Flavin-N5-oxide: a new, catalytic motif in flavoenzymology. *Arch. Biochem. Biophys.* 632, 4–10. <https://doi.org/10.1016/j.abb.2017.08.001>.
- Adak, S., Begley, T.P., 2017b. RutA-catalyzed oxidative cleavage of the uracil amide involves formation of a flavin-N5-oxide. *Biochemistry* 56, 3708–3709. <https://doi.org/10.1021/acs.biochem.7b00493>.
- Adak, S., Begley, T.P., 2019a. Flavin-N5-oxide intermediates in dibenzothiophene, uracil, and hexachlorobenzene catabolism. *New Approach. Flavin Catal.* 620, 455–468. <https://doi.org/10.1016/bs.mie.2019.03.020>.
- Adak, S., Begley, T.P., 2019b. Hexachlorobenzene catabolism involves a nucleophilic aromatic substitution and flavin-N5-oxide formation. *Biochemistry* 58, 1181–1183. <https://doi.org/10.1021/acs.biochem.9b00012>.
- Agarwal, V., El Gamal, A.A., Yamanaka, K., Poth, D., Kersten, R.D., Schorn, M., Allen, E. E., Moore, B.S., 2014. Biosynthesis of polybrominated aromatic organic compounds by marine bacteria. *Nat. Chem. Biol.* 10, 640–647. <https://doi.org/10.1038/nchembio.1564>.
- Agarwal, V., Miles, Z.D., Winter, J.M., Eustaquio, A.S., El Gamal, A.A., Moore, B.S., 2017. Enzymatic halogenation and dehalogenation reactions: pervasive and mechanistically diverse. *Chem. Rev.* 117, 5619–5674. <https://doi.org/10.1021/acs.chemrev.6b00571>.
- Agniswamy, J., Reis, R.A.G., Wang, Y.F., Smitherman, C., Su, D., Weber, I., Gadda, G., 2018. Crystal structure of yeast nitronate monooxygenase from *Cyberlindnera saturnus*. *Proteins* 86, 599–605. <https://doi.org/10.1002/prot.25470>.
- Al Fahad, A., Abood, A., Fisch, K.M., Osipow, A., Davison, J., Avramovic, M., Butts, C.P., Piel, J., Simpson, T.J., Cox, R.J., 2014. Oxidative dearomatization: the key step of sorbicillinoid biosynthesis. *Chem. Sci.* 5, 523–527. <https://doi.org/10.1039/c3sc52911h>.
- Alfieri, A., Persini, F., Ruangchan, N., Prongjit, M., Chaiyen, P., Mattevi, A., 2007. Structure of the monooxygenase component of a two-component flavoprotein monooxygenase. *Proc. Natl. Acad. Sci.* 104, 1177–1182. <https://doi.org/10.1073/pnas.0608381104>.
- Alfieri, A., Malito, E., Orru, R., Fraaije, M.W., Mattevi, A., 2008. Revealing the moonlighting role of NADP in the structure of a flavin-containing monooxygenase. *Proc. Natl. Acad. Sci.* 105, 6572–6577. <https://doi.org/10.1073/pnas.0800859105>.
- Alphand, V., Carrea, G., Wohlgenuth, R., Furstoss, R., Woodley, J.M., 2003. Towards large-scale synthetic applications of Baeyer-Villiger monooxygenases. *Trends Biotechnol.* 21, 318–323. [https://doi.org/10.1016/S0167-7799\(03\)00144-6](https://doi.org/10.1016/S0167-7799(03)00144-6).
- Andorfer, M.C., Lewis, J.C., 2018. Understanding and improving the activity of flavin-dependent halogenases via random and targeted mutagenesis. *Annu. Rev. Biochem.* 87, 159–185. <https://doi.org/10.1146/annurev-biochem-062917-012042>.
- Bailleul, G., Nicoll, C.R., Mascotti, M.L., Mattevi, A., Fraaije, M.W., 2021. Ancestral reconstruction of mammalian FMO1 enables structural determination, revealing unique features that explain its catalytic properties. *J. Biol. Chem.* 296 <https://doi.org/10.1074/jbc.RA120.016297>. In Press.
- Baker Dockrey, S.A., Narayan, A.R.H., 2020. Photocatalytic oxidative dearomatization of orcinoldehyde derivatives. *Org. Lett.* 22, 3712–3716. <https://doi.org/10.1021/acs.orglett.0c01207>.
- Baker Dockrey, S.A., Lukowski, A.L., Becker, M.R., Narayan, A.R.H., 2018. Biocatalytic site- and enantioselective oxidative dearomatization of phenols. *Nat. Chem.* 10, 119–125. <https://doi.org/10.1038/Nchem.2879>.
- Baker Dockrey, S.A., Doyon, T.J., Perkins, J.C., Narayan, A.R.H., 2019. Whole-cell biocatalysis platform for gram-scale oxidative dearomatization of phenols. *Chem. Biol. Drug Des.* 93, 1207–1213. <https://doi.org/10.1111/cbdd.13443>.
- Baldwin, C.V.F., Wohlgenuth, R., Woodley, J.M., 2008. The first 200-L scale asymmetric Baeyer-Villiger oxidation using a whole-cell biocatalyst. *Org. Process Res. Dev.* 12, 660–665. <https://doi.org/10.1021/op800046t>.
- Balke, K., Kadow, M., Mallin, H., Sass, S., Bornscheuer, U.T., 2012. Discovery, application and protein engineering of Baeyer-Villiger monooxygenases for organic synthesis. *Org. Biomol. Chem.* 10, 6249–6265. <https://doi.org/10.1039/c2ob25704a>.
- Ballou, D.P., Entsch, B., 2013. The reaction mechanisms of groups A and B flavoprotein monooxygenases. In: *Handbook of Flavoproteins: Complex Flavoproteins, Dehydrogenases and Physical Methods 2*, pp. 1–28. <https://doi.org/10.1515/9783110298345>.
- Baron, R., Riley, C., Chenprakhon, P., Thotsaporn, K., Winter, R.T., Alfieri, A., Forneris, F., van Berkel, W.J.H., Chaiyen, P., Fraaije, M.W., Mattevi, A., McCammon, J.A., 2009. Multiple pathways guide oxygen diffusion into flavoenzyme active sites. *Proc. Natl. Acad. Sci.* 106, 10603–10608. <https://doi.org/10.1073/pnas.0903809106>.
- Beam, M.P., Bosserman, M.A., Noinaj, N., Wehenkel, M., Rohr, J., 2009. Crystal structure of Baeyer-Villiger monooxygenase MtmOIV, the key enzyme of the mithramycin biosynthetic pathway. *Biochemistry* 48, 4476–4487. <https://doi.org/10.1021/bi8023509>.
- Beaty, N.B., Ballou, D.P., 1981a. The oxidative half-reaction of liver microsomal FAD-containing monooxygenase. *J. Biol. Chem.* 256, 4619–4625.
- Beaty, N.B., Ballou, D.P., 1981b. The reductive half-reaction of liver microsomal FAD-containing monooxygenase. *J. Biol. Chem.* 256, 4611–4618.
- Beaupre, B.A., Moran, G.R., 2020. N5 is the new C4a: biochemical functionalization of reduced flavins at the N5 position. *Front. Mol. Biosci.* 7, 598912. <https://doi.org/10.3389/fmolb.2020.598912>.
- Beecher, J., Willetts, A., 1998. Biotransformation of organic sulfides. Predictive active site models for sulfoxidation catalysed by 2,5-diketocamphane 1,2-monooxygenase and 3,6-diketocamphane 1,6-monooxygenase, enantiocomplementary enzymes from *Pseudomonas putida* NCIMB 10007. *Tetrahedron Asymmetry* 9, 1899–1916. [https://doi.org/10.1016/S0957-4166\(98\)00174-8](https://doi.org/10.1016/S0957-4166(98)00174-8).
- Bitto, E., Huang, Y., Bingman, C.A., Singh, S., Thorson, J.S., Phillips, G.N., 2008. The structure of flavin-dependent tryptophan 7-halogenase RebH. *Proteins* 70, 289–293. <https://doi.org/10.1002/prot.21627>.
- Bong, Y.K., Clay, M.D., Collier, S.J., Mijts, B., Vogel, M., Zhang, X., Zhu, J., Nazor, J., Smith, D., Song, S., 2011. Synthesis of prazole compounds. In: *Organization, W.I.P. (Ed.) C12N 9/02 ed.*
- Bong, Y.K., Song, S.W., Nazor, J., Vogel, M., Widegren, M., Smith, D., Collier, S.J., Wilson, R., Palanivel, S.M., Narayanaswamy, K., Mijts, B., Clay, M.D., Fong, R., Colbeck, J., Appaswami, A., Muley, S., Zhu, J., Zhang, X.Y., Liang, J., Entwistle, D., 2018. Baeyer-Villiger monooxygenase-mediated synthesis of esomeprazole as an alternative for Kagan sulfoxidation. *J. Organomet. Chem.* 83, 7453–7458. <https://doi.org/10.1021/acs.joc.8b00468>.
- Boonmak, C., Takahashi, Y., Morikawa, M., 2014. Cloning and expression of three *ladA*-type alkane monooxygenase genes from an extremely thermophilic alkane-degrading bacterium *Geobacillus thermoleovorans* B23. *Extremophiles* 18, 515–523. <https://doi.org/10.1007/s00792-014-0636-y>.
- Bordewick, S., Beier, A., Balke, K., Bornscheuer, U.T., 2018. Baeyer-Villiger monooxygenases from *Yarrowia lipolytica* catalyze preferentially sulfoxidations. *Enzym. Microb. Technol.* 109, 31–42. <https://doi.org/10.1016/j.enzmictec.2017.09.008>.
- Bosserman, M.A., Downey, T., Noinaj, N., Buchanan, S.K., Rohr, J., 2013. Molecular insight into substrate recognition and catalysis of Baeyer-Villiger monooxygenase MtmOIV, the key frame-modifying enzyme in the biosynthesis of anticancer agent mithramycin. *ACS Chem. Biol.* 8, 2466–2477. <https://doi.org/10.1021/cb400399b>.
- Bradshaw, W.H., Conrad, H.E., Corey, E.J., Gunsalus, I.C., Lednicer, D., 1959. Microbiological degradation of (+)-camphor. *J. Am. Chem. Soc.* 81, 5507. <https://doi.org/10.1021/ja01529a060>.
- Branchaud, B.P., Walsh, C.T., 1985. Functional-group diversity in enzymatic oxygenation reactions catalyzed by bacterial flavin-containing cyclohexanone oxygenase. *J. Am. Chem. Soc.* 107, 2153–2161. <https://doi.org/10.1021/ja00293a054>.
- Bregman-Cohen, A., Deri, B., Maimon, S., Pazy, Y., Fishman, A., 2018. Altering 2-hydroxybiphenyl 3-monooxygenase regioselectivity by protein engineering for the production of a new antioxidant. *ChemBioChem* 19, 583–590. <https://doi.org/10.1002/cbic.201700648>.
- Brown, A.J., Chua, N.K., Yan, N., 2019. The shape of human squalene epoxidase expands the arsenal against cancer. *Nat. Commun.* 10, 888. <https://doi.org/10.1038/s41467-019-08866-y>.
- Bruender, N.A., Thoden, J.B., Kaur, M., Avey, M.K., Holden, H.M., 2010. Molecular architecture of a C-3'-methyltransferase involved in the biosynthesis of D-tetronitron. *Biochemistry* 49, 5891–5898. <https://doi.org/10.1021/bi100782b>.
- Bruice, T.C., 1984. Oxygen-flavin chemistry. *Isr. J. Chem.* 24, 54–61. <https://doi.org/10.1002/jch.198400008>.
- Buch, K., Stransky, H., Hager, A., 1995. FAD is a further essential cofactor of the NAD(P) H and O₂-dependent zeaxanthin-epoxidase. *FEBS Lett.* 376, 45–48. [https://doi.org/10.1016/0014-5793\(95\)01243-9](https://doi.org/10.1016/0014-5793(95)01243-9).
- Bucko, M., Gemeiner, P., Schenkmyerova, A., Krajcovic, T., Rudroff, F., Mihovilovic, M. D., 2016. Baeyer-Villiger oxidations: biotechnological approach. *Appl. Microbiol. Biotechnol.* 100, 6585–6599. <https://doi.org/10.1007/s00253-016-7670-x>.
- Campbell, A.C., Robinson, R., Mena-Aguilar, D., Sobrado, P., Tanner, J.J., 2020a. Structural determinants of flavin dynamics in a class B monooxygenase. *Biochemistry* 59, 4609–4616. <https://doi.org/10.1021/acs.biochem.0c00783>.
- Campbell, A.C., Stiers, K.M., Del Campo, J.S.M., Mehra-Chaudhary, R., Sobrado, P., Tanner, J.J., 2020b. Trapping conformational states of a flavin-dependent N-monooxygenase *in crystallo* reveals protein and flavin dynamics. *J. Biol. Chem.* 295, 13239–13249. <https://doi.org/10.1074/jbc.RA120.014750>.
- Cao, H.Y., Wang, P., Peng, M., Shao, X., Chen, X.L., Li, C.Y., 2018. Crystal structure of the dimethylsulfide monooxygenase DmoA from *Hyphomicrobium sulfonivorans*. *Acta Crystallogr. F* 74, 781–786. <https://doi.org/10.1107/S2053230x18015844>.
- Cao, X., Yang, H.L., Shang, C.Q., Ma, S., Liu, L., Cheng, J.L., 2019. The roles of auxin biosynthesis YUCCA gene family in plants. *Int. J. Mol. Sci.* 20, 6343. <https://doi.org/10.3390/ijms20246343>.
- Cashman, J.R., Zhang, J., 2006. Human flavin-containing monooxygenases. *Annu. Rev. Pharmacol. Toxicol.* 46, 65–100. <https://doi.org/10.1146/annurev.pharmtox.46.120604.141043>.
- Catucci, G., Gao, C.L., Sadeghi, S.J., Gilardi, G., 2017. Chemical applications of Class B flavoprotein monooxygenases. *Rend. Lincei Sci. Fis. Nat.* 28, 195–206. <https://doi.org/10.1007/s12210-016-0583-x>.
- Catucci, G., Gilardi, G., Sadeghi, S.J., 2020. Production of drug metabolites by human FMO3 in *Escherichia coli*. *Microb. Cell Factories* 19, 74. <https://doi.org/10.1186/s12934-020-01332-1>.

- Kubitza, C., Faust, A., Gutt, M., Gath, L., Ober, D., Scheidig, A.J., 2018. Crystal structure of pyrrolizidine alkaloid *N*-oxygenase from the grasshopper *Zonocerus variegatus*. *Acta Crystallogr. D* 74, 422–432. <https://doi.org/10.1107/S2059798318003510>.
- Kugel, S., Baunach, M., Baer, P., Ishida-Ito, M., Sundaram, S., Xu, Z.L., Groll, M., Hertweck, C., 2017. Cryptic indole hydroxylation by a non-canonical terpenoid cyclase parallels bacterial xenobiotic detoxification. *Nat. Commun.* 8, 15804. <https://doi.org/10.1038/ncomms15804>.
- Latham, J., Brandenburger, E., Shepherd, S.A., Menon, B.R.K., Mickfield, J., 2018. Development of halogenase enzymes for use in synthesis. *Chem. Rev.* 118, 232–269. <https://doi.org/10.1021/acs.chemrev.7b00032>.
- Leisch, H., Morley, K., Lau, P.C.K., 2011. Baeyer-Villiger monooxygenases: more than just green chemistry. *Chem. Rev.* 111, 4165–4222. <https://doi.org/10.1021/cr1003437>.
- Li, J., Hansen, B.G., Ober, J.A., Kliebenstein, D.J., Halkier, B.A., 2008. Subclade of flavin monooxygenases involved in aliphatic glucosinolate biosynthesis. *Plant Physiol.* 148, 1721–1733. <https://doi.org/10.1104/pp.108.125757>.
- Li, G.Y., Fürst, M.J.L.J., Mansouri, H.R., Resmann, A.K., Ilie, A., Rudroff, F., Mihovilovic, M.D., Fraaije, M.W., Reetz, M.T., 2017. Manipulating the stereoselectivity of the thermostable Baeyer-Villiger monooxygenase TmCHMO by directed evolution. *Org. Biomol. Chem.* 15, 9824–9829. <https://doi.org/10.1039/c7ob02692g>.
- Li, G.Y., Garcia-Borràs, M., Fürst, M.J.L.J., Ilie, A., Fraaije, M.W., Houk, K.N., Reetz, M.T., 2018. Overriding traditional electronic effects in biocatalytic Baeyer-Villiger reactions by directed evolution. *J. Am. Chem. Soc.* 140, 10464–10472. <https://doi.org/10.1021/8b04742>.
- Lin, Z., Ji, J., Zhou, S., Zhang, F., Wu, J., Guo, Y., Liu, W., 2017. Processing 2-methyl-L-tryptophan through tandem transamination and selective oxygenation initiates indole ring expansion in the biosynthesis of thioestrep. *J. Am. Chem. Soc.* 139, 12105–12108. <https://doi.org/10.1021/jacs.7b05337>.
- Lin, K.H., Lyu, S.Y., Yeh, H.W., Li, Y.S., Hsu, N.S., Huang, C.M., Wang, Y.L., Shih, H.W., Wang, Z.C., Wu, C.J., Li, T.L., 2020. Structural and chemical trapping of flavin-oxide intermediates reveals substrate-directed reaction multiplicity. *Protein Sci.* 29, 1655–1666. <https://doi.org/10.1002/pro.3879>.
- Liu, L.K., Abdelwahab, H., Del Campo, J.S.M., Mehra-Chaudhary, R., Sobrado, P., Tanner, J.J., 2016. The structure of the antibiotic deactivating, *N*-hydroxylating rifampicin monooxygenase. *J. Biol. Chem.* 291, 21553–21562. <https://doi.org/10.1074/jbc.M116.745315>.
- Liu, L.K., Dai, Y., Abdelwahab, H., Sobrado, P., Tanner, J.J., 2018. Structural evidence for rifampicin monooxygenase inactivating rifampicin by cleaving its ansa-bridge. *Biochemistry* 57, 2065–2068. <https://doi.org/10.1021/acs.biochem.8b00190>.
- Lockridge, O., Massey, V., Sullivan, P.A., 1972. Mechanism of action of flavoenzyme lactate oxidase. *J. Biol. Chem.* 247, 8097–8106.
- Loncar, N., Fiorentini, F., Baillieu, G., Savino, S., Romero, E., Mattevi, A., Fraaije, M.W., 2019. Characterization of a thermostable flavin-containing monooxygenase from *Nitrocola lacinisaponensis* (NiFMO). *Appl. Microbiol. Biotechnol.* 103, 1755–1764. <https://doi.org/10.1007/s00253-018-09579-w>.
- Lutz, J., Mozhaev, V.V., Kholmitsky, Y.L., Witholt, B., Schmid, A., 2002. Preparative application of 2-hydroxybiphenyl 3-monooxygenase with enzymatic cofactor regeneration in organic-aqueous reaction media. *J. Mol. Catal. B Enzym.* 19, 177–187. [https://doi.org/10.1016/S1381-1177\(02\)00165-0](https://doi.org/10.1016/S1381-1177(02)00165-0).
- Lyu, S.-Y., Lin, K.H., Yeh, H.W., Li, Y.S., Huang, C.M., Wang, Y.L., Shih, H.W., Hsu, N.S., Wu, C.J., Li, T.L., 2019. The flavin mononucleotide cofactor in α -hydroxyacid oxidases exerts its electrophilic/nucleophilic duality in control of the substrate-oxidation level. *Acta Crystallogr. D* 75, 918–929. <https://doi.org/10.1107/S2059798319011938>.
- Maczka, W., Winska, K., Grabarczyk, M., 2018. Biotechnological methods of sulfoxidation: yesterday, today, tomorrow. *Catalysts* 8, 624. <https://doi.org/10.3390/catal8120624>.
- Maeda-Yorita, K., Aki, K., Sagai, H., Misaki, H., Massey, V., 1995. L-Lactate oxidase and L-lactate monooxygenase: mechanistic variations on a common structural theme. *Biochimie* 77, 631–642. [https://doi.org/10.1016/0300-9084\(96\)88178-8](https://doi.org/10.1016/0300-9084(96)88178-8).
- Malito, E., Alfieri, A., Fraaije, M.W., Mattevi, A., 2004. Crystal structure of a Baeyer-Villiger monooxygenase. *Proc. Natl. Acad. Sci.* 101, 13157–13162. <https://doi.org/10.1073/pnas.0404538101>.
- Mascotti, M.L., Ayub, M.J., Dudek, H., Sanz, M.K., Fraaije, M.W., 2013. Cloning, overexpression and biocatalytic exploration of a novel Baeyer-Villiger monooxygenase from *Aspergillus fumigatus* Af293. *AMB Express* 3, 33. <https://doi.org/10.1186/2191-0855-3-33>.
- Mascotti, M.L., Lapadula, W.J., Ayub, M.J., 2015. The origin and evolution of Baeyer-Villiger monooxygenases (BVMOs): an ancestral family of flavin monooxygenases. *PLoS One* 10, e0132689. <https://doi.org/10.1371/journal.pone.0132689>.
- Mascotti, M.L., Ayub, M.J., Furnham, N., Thornton, J.M., Laskowski, R.A., 2016. Chopping and changing: the evolution of the flavin-dependent monooxygenases. *J. Mol. Biol.* 428, 3131–3146. <https://doi.org/10.1016/j.jmb.2016.07.003>.
- Mashiguchi, K., Tanaka, K., Sakai, T., Sugawara, S., Kawaide, H., Natsume, M., Hanada, A., Yaeno, T., Shirasu, K., Yao, H., McSteen, P., Zhao, Y.D., Hayashi, K., Kamiya, Y., Kasahara, H., 2011. The main auxin biosynthesis pathway in *Arabidopsis*. *Proc. Natl. Acad. Sci.* 108, 18512–18517. <https://doi.org/10.1073/pnas.1108434108>.
- Massey, V., 1994. Activation of molecular oxygen by flavins and flavoproteins. *J. Biol. Chem.* 269, 22459–22462.
- Matsuda, K., Tomita, T., Shin-ya, K., Wakimoto, T., Kuzuyama, T., Nishiyama, M., 2018. Discovery of unprecedented hydrazine-forming machinery in bacteria. *J. Am. Chem. Soc.* 140, 9083–9086. <https://doi.org/10.1021/jacs.8b05354>.
- Matsui, D., Im, D.H., Sugawara, A., Fukuta, Y., Fushinobu, S., Isobe, K., Asano, Y., 2014. Mutational and crystallographic analysis of L-amino acid oxidase/monooxygenase from *Pseudomonas* sp. AIU 813: Interconversion between oxidase and monooxygenase activities. *FEBS Open Biol.* 4, 220–228. <https://doi.org/10.1016/j.fob.2014.02.002>.
- Matsushita, T., Kishimoto, S., Hara, K., Hashimoto, H., Watanabe, K., 2020. Structural and functional analyses of a spiro-carbon-forming, highly promiscuous epoxidase from fungal natural product biosynthesis. *Biochemistry* 59, 4787–4792. <https://doi.org/10.1021/acs.biochem.0c00896>.
- Matthews, A., Saleem-Batcha, R., Sanders, J.N., Stull, F., Houk, K.N., Teufel, R., 2020. Aminoperoxide adducts expand the catalytic repertoire of flavin monooxygenases. *Nat. Chem. Biol.* 16, 556–563. <https://doi.org/10.1038/s41589-020-0476-2>.
- McGhie, E.J., Littlechild, J.A., 1996. The purification and crystallisation of 2,5-diketocamphane 1,2-monooxygenase and 3,6-diketocamphane 1,6-monooxygenase from *Pseudomonas putida* NCIMB 10007. *Biochem. Soc. Trans.* 24, S29. <https://doi.org/10.1042/bst024029s>.
- McGhie, E.J., Isupov, M.N., Schroder, E., Littlechild, J.A., 1998. Crystallization and preliminary X-ray diffraction studies of the oxygenating subunit of 3,6-diketocamphane monooxygenase from *Pseudomonas putida*. *Acta Crystallogr. D* 54, 1035–1038. <https://doi.org/10.1107/S0907444998004946>.
- Messiha, H.L., Ahmed, S.T., Karuppiah, V., Suardiaz, R., Ascue Avalos, G.A., Fey, N., Yeates, S., Toogood, H.S., Mulholland, A.J., Scrutton, N.S., 2018. Biocatalytic routes to lactone monomers for polymer production. *Biochemistry* 57, 1997–2008. <https://doi.org/10.1021/acs.biochem.8b00169>.
- Meyer, A., Wursten, M., Schmid, A., Kohler, H.P.E., Witholt, B., 2002. Hydroxylation of indole by laboratory-evolved 2-hydroxybiphenyl 3-monooxygenase. *J. Biol. Chem.* 277, 34161–34167. <https://doi.org/10.1074/jbc.M205621200>.
- Milzarek, T.M., Einsiedler, M., Aldemir, H., D'Agostino, P.M., Evers, J.K., Hertrampf, G., Lamm, K., Malay, M., Matura, A., Müller, J.I., Gulder, T.A.M., 2019. Bypassing biocatalytic substrate limitations in oxidative dearomatization reactions by transient substrate mimicking. *Org. Lett.* 21, 4520–4524. <https://doi.org/10.1021/acs.orglett.9b01398>.
- Minami, A., Oguri, H., Watanabe, K., Oikawa, H., 2013. Biosynthetic machinery of ionophore polyether lasalocid: enzymatic construction of polyether skeleton. *Curr. Opin. Chem. Biol.* 17, 555–561. <https://doi.org/10.1016/j.coba.2013.06.004>.
- Minerdi, D., Zgrablic, I., Castrignano, S., Catucci, G., Medana, C., Terlizzi, M.E., Griboudo, G., Gilardi, G., Sadeghi, S.J., 2016. *Escherichia coli* overexpressing a Baeyer-Villiger monooxygenase from *Acinetobacter radioresistens* becomes resistant to imipenem. *Antimicrob. Agents Chemother.* 60, 64–74. <https://doi.org/10.1128/AAC.01088-15>.
- Mirza, I.A., Yachnin, B.J., Wang, S.Z., Grosse, S., Bergeron, H., Imura, A., Iwaki, H., Hasegawa, Y., Lau, P.C.K., Berghuis, A.M., 2009. Crystal structures of cyclohexanone monooxygenase reveal complex domain movements and a sliding cofactor. *J. Am. Chem. Soc.* 131, 8848–8854. <https://doi.org/10.1021/ja910578>.
- Mohamed, M.E.S., Al-Yacoub, Z.H., Vedakumar, J.V., 2015. Biocatalytic desulfurization of thiophenic compounds and crude oil by newly isolated bacteria. *Front. Microbiol.* 6, 112. <https://doi.org/10.3389/fmicb.2015.00112>.
- Mondal, D., Fisher, B.F., Jiang, Y., Lewis, J.C., 2020. Flavin-dependent halogenases catalyze enantioselective olefin halocyclization. *ChemRxiv*. <https://doi.org/10.26434/chemrxiv.12982433.v1>.
- Montersino, S., Tischler, D., Gassner, G.T., van Berkel, W.J.H., 2011. Catalytic and structural features of flavoprotein hydroxylases and epoxidases. *Adv. Synth. Catal.* 353, 2301–2319. <https://doi.org/10.1002/adsc.201100384>.
- Montersino, S., Orru, R., Barendregt, A., Westphal, A.H., van Duijn, E., Mattevi, A., van Berkel, W.J.H., 2013. Crystal structure of 3-hydroxybenzoate 6-hydroxylase uncovers lipid-assisted flavoprotein strategy for regioselective aromatic hydroxylation. *J. Biol. Chem.* 288, 26235–26245. <https://doi.org/10.1074/jbc.M113.479303>.
- Moonen, M.J.H., Westphal, A.H., Rietjens, I.M.C.M., van Berkel, W.J.H., 2005. Enzymatic Baeyer-Villiger oxidation of benzaldehydes. *Adv. Synth. Catal.* 347, 1027–1034. <https://doi.org/10.1002/adsc.200404307>.
- Morgan, K.D., Andersen, R.J., Ryan, K.S., 2019. Piperazine acid-containing natural products: structures and biosynthesis. *Nat. Prod. Rep.* 36, 1628–1653. <https://doi.org/10.1039/c8np00076j>.
- Moriwaki, Y., Yato, M., Terada, T., Saito, S., Nukui, N., Iwasaki, T., Nishi, T., Kawaguchi, Y., Okamoto, K., Arakawa, T., Yamada, C., Fushinobu, S., Shimizu, K., 2019. Understanding the molecular mechanism underlying the high catalytic activity of *p*-hydroxybenzoate hydroxylase mutants for producing gallic acid. *Biochemistry* 58, 4543–4558. <https://doi.org/10.1021/acs.biochem.9b00443>.
- Morrison, E., Kantz, A., Gassner, G.T., Sazinsky, M.H., 2013. Structure and mechanism of styrene monooxygenase reductase: new insight into the FAD-transfer reaction. *Biochemistry* 52, 6063–6075. <https://doi.org/10.1021/Bi400763h>.
- Mügge, C., Heine, T., Baraibar, A.G., van Berkel, W.J.H., Paul, C.E., Tischler, D., 2020. Flavin-dependent *N*-hydroxylating enzymes: distribution and application. *Appl. Microbiol. Biotechnol.* 104, 6481–6499. <https://doi.org/10.1007/s00253-020-10705-w>.
- Müller, F., 1985. Flavin-dependent hydroxylases. *Biochem. Soc. Trans.* 13, 443–447. <https://doi.org/10.1042/bst0130443>.
- Müller, F., 1987. Flavin radicals: chemistry and biochemistry. *Free Radic. Biol. Med.* 3, 215–230. [https://doi.org/10.1016/0891-5849\(87\)90009-8](https://doi.org/10.1016/0891-5849(87)90009-8).
- Müller, F., 2014. NMR spectroscopy on flavins and flavoproteins. In: Weber, S., Schleicher, E. (Eds.), *Flavins and Flavoproteins: Methods and Protocols*. Springer New York, New York, NY, pp. 229–306.
- Nakamoto, K.D., Perkins, S.W., Campbell, R.G., Bauerle, M.R., Gerwig, T.J., Gerishioglu, S., Wesdemiotis, C., Anderson, M.A., Hicks, K.A., Snider, M.J., 2019. Mechanism of 6-hydroxynicotinate 3-monooxygenase, a flavin-dependent decarboxylative hydroxylase involved in bacterial nicotinic acid degradation. *Biochemistry* 58, 1751–1763. <https://doi.org/10.1021/acs.biochem.8b00969>.

- Nakano, H., Wieser, M., Hurh, B., Kawai, T., Yoshida, T., Yamane, T., Nagasawa, T., 1999. Purification, characterization and gene cloning of 6-hydroxynicotinate 3-monooxygenase from *Pseudomonas fluorescens* TN5. *Eur. J. Biochem.* 260, 120–126. <https://doi.org/10.1046/j.1432-1327.1999.00124.x>.
- Neubauer, P.R., Widmann, C., Wibberg, D., Schroder, L., Frese, M., Kottke, T., Kalinowski, J., Niemann, H.H., Sewald, N., 2018. A flavin-dependent halogenase from metagenomic analysis prefers bromination over chlorination. *PLoS One* 13, e0196797. <https://doi.org/10.1371/journal.pone.0196797>.
- Neumann, C.S., Jiang, W., Heemstra, J.R., Gontang, E.A., Kolter, R., Walsh, C.T., 2012. Biosynthesis of piperazine acid via N⁵-hydroxy-ornithine in *Kutzneria* spp. 744. *ChemBioChem* 13, 972–976. <https://doi.org/10.1002/cbic.201200054>.
- Nicoll, C.R., Baillieu, G., Fiorentini, F., Mascotti, M.L., Fraaije, M.W., Mattevi, A., 2020. Ancestral-sequence reconstruction unveils the structural basis of function in mammalian FMOs. *Nat. Struct. Mol. Biol.* 27, 14–24. <https://doi.org/10.1038/s41594-019-0347-2>.
- Nijvipakul, S., Wongratana, J., Suadee, C., Entsch, B., Ballou, D.P., Chaiyen, P., 2008. LuxG is a functioning flavin reductase for bacterial luminescence. *J. Bacteriol.* 190, 1531–1538. <https://doi.org/10.1128/Jb.01660-07>.
- Ohnishi, T., Yamamoto, S., Hayashida, O., Izumi, T., Shiba, T., 1976. Studies on reaction specificity of flavoprotein lysine monooxygenase with modified substrates. *Arch. Biochem. Biophys.* 176, 358–365. [https://doi.org/10.1016/0003-9861\(76\)90175-2](https://doi.org/10.1016/0003-9861(76)90175-2).
- Olucha, J., Meneely, K.M., Chilton, A.S., Lamb, A.L., 2011. Two structures of an N-hydroxylating flavoprotein monooxygenase ornithine hydroxylase from *Pseudomonas aeruginosa*. *J. Biol. Chem.* 286, 31789–31798. <https://doi.org/10.1074/jbc.M111.265876>.
- Opperman, D.J., Reetz, M.T., 2010. Towards practical Baeyer-Villiger-monoxygenases: design of cyclohexanone monooxygenase mutants with enhanced oxidative stability. *ChemBioChem* 11, 2589–2596. <https://doi.org/10.1002/cbic.201000464>.
- Padyana, A.K., Gross, S., Jin, L., Gianchetta, G., Narayanaswamy, R., Wang, F., Wang, R., Fang, C., Lv, X.B., Biller, S.A., Dang, L., Mahoney, C.E., Nagaraja, N., Pirman, D., Sui, Z.H., Popovici-Muller, J., Smolen, G.A., 2019. Structure and inhibition mechanism of the catalytic domain of human squalene epoxidase. *Nat. Commun.* 10, 97. <https://doi.org/10.1038/s41467-018-07928-x>.
- Palfey, B.A., Moran, G.R., Entsch, B., Ballou, D.P., Massey, V., 1999. Substrate recognition by "password" in p-hydroxybenzoate hydroxylase. *Biochemistry* 38, 1153–1158. <https://doi.org/10.1021/Bi9826613>.
- Panke, S., Wubolts, M.G., Schmid, A., Witholt, B., 2000. Production of enantiopure styrene oxide by recombinant *Escherichia coli* synthesizing a two-component styrene monooxygenase. *Biotechnol. Bioeng.* 69, 91–100. [https://doi.org/10.1002/\(Sici\)1097-0290\(20000705\)69:1<91::Aid-Bit1>3.0.Co;2-X](https://doi.org/10.1002/(Sici)1097-0290(20000705)69:1<91::Aid-Bit1>3.0.Co;2-X).
- Panke, S., Held, M., Wubolts, M.G., Witholt, B., Schmid, A., 2002. Pilot-scale production of (S)-styrene oxide from styrene by recombinant *Escherichia coli* synthesizing styrene monooxygenase. *Biotechnol. Bioeng.* 80, 33–41. <https://doi.org/10.1002/Biot.10346>.
- Parniak, M.A., Jackson, G.E., Murray, G.J., Viswanatha, T., 1979. Studies on the formation of N⁶-hydroxyllysine in cell-free extracts of *Aerobacter aerogenes* 62-1. *Biochim. Biophys. Acta* 569, 99–108. [https://doi.org/10.1016/0005-2744\(79\)90085-8](https://doi.org/10.1016/0005-2744(79)90085-8).
- Parry, R.J., Li, W.Y., 1997. An NADPH:FAD oxidoreductase from the valaninycin producer, *Streptomyces viridifaciens*. *J. Biol. Chem.* 272, 23303–23311. <https://doi.org/10.1074/jbc.272.37.23303>.
- Paul, C.E., Tischler, D., Riedel, A., Heine, T., Itoh, N., Hollmann, F., 2015. Nonenzymatic regeneration of styrene monooxygenase for catalysis. *ACS Catal.* 5, 2961–2965. <https://doi.org/10.1021/acscatal.5b00041>.
- Payne, J.W., Bolton, H., Campbell, J.A., Xun, L.Y., 1998. Purification and characterization of EDTA monooxygenase from the EDTA-degrading bacterium BNC1. *J. Bacteriol.* 180, 3823–3827. <https://doi.org/10.1128/Jb.180.15.3823-3827.1998>.
- Pelosi, L., Ducluzeau, A.L., Loiseau, L., Barras, F., Schneider, D., Junier, I., Pierrel, F., 2016. Evolution of ubiquinone biosynthesis: multiple proteobacterial enzymes with various regioselectivities to catalyze three contiguous aromatic hydroxylation reactions. *Msystems* 1. <https://doi.org/10.1128/mSystems.00091-16.e00091-00016>.
- Phillips, I.R., Shephard, E.A., 2019. Endogenous roles of mammalian flavin-containing monooxygenases. *Catalysts* 9, 1001. <https://doi.org/10.3390/catal9121001>.
- Phonbuppha, J., Tinikul, R., Wongnate, T., Intasian, P., Hollmann, F., Paul, C.E., Chaiyen, P., 2020. A minimized chemoenzymatic cascade for bacterial luciferase in bioreporter applications. *ChemBioChem* 21, 2073–2079. <https://doi.org/10.1002/cbic.202000100>.
- Piano, V., Palfey, B.A., Mattevi, A., 2017. Flavins as covalent catalysts: new mechanisms emerge. *Trends Biochem. Sci.* 42, 457–469. <https://doi.org/10.1016/j.tibs.2017.02.005>.
- Pimviriyakul, P., Chaiyen, P., 2018. A complete bioconversion cascade for dehalogenation and denitration by bacterial flavin-dependent enzymes. *J. Biol. Chem.* 293, 18525–18539. <https://doi.org/10.1074/jbc.RA118.005538>.
- Pimviriyakul, P., Thotsaporn, K., Sucharitakul, J., Chaiyen, P., 2017. Kinetic mechanism of the dechlorinating flavin-dependent monooxygenase HadA. *J. Biol. Chem.* 292, 4818–4832. <https://doi.org/10.1074/jbc.M116.774448>.
- Pitsawong, W., Chenprakhon, P., Dhammaraj, T., Medhanavyn, D., Sucharitakul, J., Tongsook, C., van Berkel, W.J.H., Chaiyen, P., Miller, A.F., 2020. Tuning of pKa values activates substrates in flavin-dependent aromatic hydroxylases. *J. Biol. Chem.* 295, 3965–3981. <https://doi.org/10.1074/jbc.RA119.011884>.
- Podzelinska, K., Latimer, R., Bhattacharya, A., Vining, L.C., Zechel, D.L., Jia, Z.C., 2010. Chlorophenolic biosynthesis: the structure of CmlS, a flavin-dependent halogenase showing a covalent flavin-aspartate bond. *J. Mol. Biol.* 397, 316–331. <https://doi.org/10.1016/j.jmb.2010.01.020>.
- Ralph, E.C., Anderson, M.A., Cleland, W.W., Fitzpatrick, P.F., 2006. Mechanistic studies of the flavoenzyme tryptophan 2-monooxygenase: deuterium and ¹⁵N kinetic isotope effects on alanine oxidation by an L-amino acid oxidase. *Biochemistry* 45, 15844–15852. <https://doi.org/10.1021/bi061894o>.
- Reetz, M.T., 2009. Directed evolution of enantioselective enzymes: an unconventional approach to asymmetric catalysis in organic chemistry. *J. Organomet. Chem.* 74, 5767–5778. <https://doi.org/10.1021/Jo901046k>.
- Reetz, M.T., Wu, S., 2008. Greatly reduced amino acid alphabets in directed evolution: making the right choice for saturation mutagenesis at homologous enzyme positions. *Chem. Commun.* 5499–5501. <https://doi.org/10.1039/b813388c>.
- Reetz, M.T., Wu, S., 2009. Laboratory evolution of robust and enantioselective Baeyer-Villiger monooxygenases for asymmetric catalysis. *J. Am. Chem. Soc.* 131, 15424–15432. <https://doi.org/10.1021/Ja906212k>.
- Ricken, B., Kolvenbach, B.A., Corvini, P.F.-X., 2015. *Ips*-substitution - the hidden gate to xenobiotic degradation pathways. *Curr. Opin. Biotechnol.* 33, 220–227. <https://doi.org/10.1016/j.copbio.2015.03.009>.
- Ricken, B., Kolvenbach, B.A., Bergesch, C., Benndorf, D., Kroll, K., Strnad, H., Vlcek, C., Adaxo, R., Hammes, F., Shahgaldian, P., Schaffer, A., Kohler, H.P.E., Corvini, P.F.X., 2017. FMN₂-dependent monooxygenases initiate catabolism of sulfonamides in *Microbacterium* sp. strain BR1 subsisting on sulfonamide antibiotics. *Sci. Rep.* 7, 15783. <https://doi.org/10.1038/s41598-017-16132-8>.
- Riebel, A., Dudek, H.M., de Gonzalo, G., Stepniak, P., Rychlewski, L., Fraaije, M.W., 2012. Expanding the set of rhodococcal Baeyer-Villiger monooxygenases by high-throughput cloning, expression and substrate screening. *Appl. Microbiol. Biotechnol.* 95, 1479–1489. <https://doi.org/10.1007/s00253-011-3823-0>.
- Riebel, A., de Gonzalo, G., Fraaije, M.W., 2013. Expanding the biocatalytic toolbox of flavoprotein monooxygenases from *Rhodococcus jostii* RHA1. *J. Mol. Catal. B Enzym.* 88, 20–25. <https://doi.org/10.1016/j.molcatb.2012.11.009>.
- Riebel, A., Fink, M.J., Mihovilovic, M.D., Fraaije, M.W., 2014. Type II flavin-containing monooxygenases: a new class of biocatalysts that harbors Baeyer-Villiger monooxygenases with a relaxed coenzyme specificity. *ChemCatChem* 6, 1112–1117. <https://doi.org/10.1002/cctc.201300550>.
- Rioz-Martínez, A., Kopacz, M., de Gonzalo, G., Torres Pazmiño, D.E., Gotor, V., Fraaije, M.W., 2011. Exploring the biocatalytic scope of a bacterial flavin-containing monooxygenase. *Org. Biomol. Chem.* 9, 1337–1341. <https://doi.org/10.1039/C0ob00988a>.
- Robbins, J.M., Ellis, H.R., 2019. Investigations of two-component flavin-dependent monooxygenase systems. *Methods Enzymol.* 399–422.
- Robinson, R.M., Sobrado, P., 2013. Flavin-dependent monooxygenases in siderophore biosynthesis. In: *Handbook of Flavoproteins: Complex Flavoproteins, Dehydrogenases and Physical Methods*, Vol 2, pp. 29–50. <https://doi.org/10.1515/9783110298345>.
- Rodríguez Benítez, A., Tweedy, S., Baker Dockrey, S.A., Lukowski, A.L., Wymore, T., Khare, D., Brooks III, C.L., Palfey, B.A., Smith, J.L., Narayan, A.R.H., 2019. Structural basis for selectivity in flavin-dependent monooxygenase-catalyzed oxidative dearomatization. *ACS Catal.* 9, 3633–3640. <https://doi.org/10.1021/acscatal.8b04575>.
- Romero, E., Castellanos, J.R.G., Mattevi, A., Fraaije, M.W., 2016. Characterization and crystal structure of a robust cyclohexanone monooxygenase. *Angew. Chem. Int. Ed.* 55, 15852–15855. <https://doi.org/10.1002/anie.201608951>.
- Romero, E., Castellanos, J.R.G., Gadda, G., Fraaije, M.W., Mattevi, A., 2018. Same substrate, many reactions: oxygen activation in flavoenzymes. *Chem. Rev.* 118, 1742–1769. <https://doi.org/10.1021/acs.chemrev.7b00650>.
- Ryerson, C.C., Ballou, D.P., Walsh, C., 1982. Mechanistic studies on cyclohexanone oxygenase. *Biochemistry* 21, 2644–2655. <https://doi.org/10.1021/bi00540a011>.
- Sadauskas, M., Statkeviciute, R., Vaitekunas, J., Meskys, R., 2020. Bioconversion of biologically active indole derivatives with indole-3-acetic acid-degrading enzymes from *Caballeronia glathei* DSM50014. *Biomolecules* 10, 663. <https://doi.org/10.3390/biom10040663>.
- Sakakibara, J., Watanabe, R., Kanai, Y., Ono, T., 1995. Molecular-cloning and expression of rat squalene epoxidase. *J. Biol. Chem.* 270, 17–20. <https://doi.org/10.1074/jbc.270.1.17>.
- Saleem-Batcha, R., Stull, F., Sanders, J.N., Moore, B.S., Palfey, B.A., Houk, K.N., Teufel, R., 2018. Enzymatic control of dioxygen binding and functionalization of the flavin cofactor. *Proc. Natl. Acad. Sci.* 115, 4909–4914. <https://doi.org/10.1073/pnas.1801189115>.
- Salvi, F., Agniswamy, J., Yuan, H.L., Vercammen, K., Pelicaen, R., Cornelis, P., Spain, J. C., Weber, I.T., Gadda, G., 2014. The combined structural and kinetic characterization of a bacterial nitronate monooxygenase from *Pseudomonas aeruginosa* PAO1 establishes NMO class I and II. *J. Biol. Chem.* 289, 23764–23775. <https://doi.org/10.1074/jbc.M114.577791>.
- Sartor, L., Ibarra, C., Al-Mestarihi, A., Bachmann, B.O., Vey, J.L., 2015. Structure of DnmZ, a nitrososynthase in the *Streptomyces peucetius* anthracycline biosynthetic pathway. *Acta Crystallogr. Sect. F* 71, 1205–1214. <https://doi.org/10.1107/S2053230x15014272>.
- Schlauch, N.L., 2007. Flavin-containing monooxygenases in plants: looking beyond detox. *Trends Plant Sci.* 12, 412–418. <https://doi.org/10.1016/j.tplants.2007.08.009>.
- Schmid, A., Hofstetter, K., Feiten, H.-J., Hollmann, F., Witholt, B., 2001. Integrated biocatalytic synthesis on gram scale: the highly enantioselective preparation of chiral oxiranes with styrene monooxygenase. *Adv. Synth. Catal.* 343, 732–737. [https://doi.org/10.1002/1615-4169\(200108\)343:6<732::Aid-ads732>3.0.Co;2-q](https://doi.org/10.1002/1615-4169(200108)343:6<732::Aid-ads732>3.0.Co;2-q).
- Schmidt, S., Bornscheuer, U.T., 2020. Baeyer-Villiger monooxygenases: from protein engineering to biocatalytic applications. In: Chaiyen, P., Tamano, F. (Eds.), *The Enzymes*. Academic Press, pp. 231–281.

- Schnepel, C., Sewald, N., 2017. Enzymatic halogenation: a timely strategy for regioselective C-H activation. *Chem. Eur. J.* 23, 12064–12086. <https://doi.org/10.1002/chem.201701209>.
- Schreuder, H.A., Prick, P.A.J., Wierenga, R.K., Vriend, G., Wilson, K.S., Hol, W.G.J., Drenth, J., 1989. Crystal structure of the *p*-hydroxybenzoate hydroxylase-substrate complex refined at 1.9 Å resolution. *J. Mol. Biol.* 208, 679–696. [https://doi.org/10.1016/0022-2836\(89\)90158-7](https://doi.org/10.1016/0022-2836(89)90158-7).
- Schreuder, H.A., Mattevi, A., Obmolova, G., Kalk, K.H., Hol, W.G.J., van der Bolt, F.J.T., van Berkel, W.J.H., 1994. Crystal structures of wild-type *p*-hydroxybenzoate hydroxylase complexed with 4-aminobenzoate, 2,4-dihydroxybenzoate, and 2-hydroxy-4-aminobenzoate and of the Tyr222Ala mutant complexed with 2-hydroxy-4-aminobenzoate. Evidence for a proton channel and a new binding mode of the flavin ring. *Biochemistry* 33, 10161–10170. <https://doi.org/10.1021/bi00199a044>.
- Schroeder, L., Frese, M., Müller, C., Sewald, N., Kottke, T., 2018. Photochemically driven biocatalysis of halogenases for the green production of chlorinated compounds. *ChemCatChem* 10, 3336–3341. <https://doi.org/10.1002/cctc.201800280>.
- Schwab, J.M., 1981. Stereochemistry of an enzymatic Baeyer-Villiger reaction. Application of deuterium NMR. *J. Am. Chem. Soc.* 103, 1876–1878. <https://doi.org/10.1021/ja00397a066>.
- Scott, J.C., Greenhut, I.V., Leveau, J.H.J., 2013. Functional characterization of the bacterial *iac* genes for degradation of the plant hormone indole-3-acetic acid. *J. Chem. Ecol.* 39, 942–951. <https://doi.org/10.1007/s10886-013-0324-x>.
- Sheng, D.W., Ballou, D.P., Massey, V., 2001. Mechanistic studies of cyclohexanone monooxygenase: chemical properties of intermediates involved in catalysis. *Biochemistry* 40, 11156–11167. <https://doi.org/10.1021/Bi011153h>.
- Sib, A., Gulder, T.A.M., 2017. Stereoselective total synthesis of bisorbicillinoid natural products by enzymatic oxidative dearomatization/dimerization. *Angew. Chem. Int. Ed.* 56, 12888–12891. <https://doi.org/10.1002/anie.201705976>.
- Sib, A., Gulder, T.A.M., 2018. Chemo-enzymatic total synthesis of oxosorbicillinol, sorrentanone, rezishanones B and C, sorbatechol A, bisvertinolone, and (+)-epoxysorbicillinol. *Angew. Chem. Int. Ed.* 57, 14650–14653. <https://doi.org/10.1002/anie.201802176>.
- Sib, A., Milzarek, T.M., Herrmann, A., Oubraham, L., Müller, J.I., Pichlmair, A., Brack-Werner, R., Gulder, T.A.M., 2019. Chemoenzymatic total synthesis of sorbatechol structural analogues and evaluation of their antiviral potential. *ChemBioChem* 21, 492–495. <https://doi.org/10.1002/cbic.201900472>.
- Smith, D.R.M., Uria, A.R., Helfrich, E.J.N., Milbredt, D., van Pée, K.-H., Piel, J., Goss, R.J.M., 2017. An unusual flavin-dependent halogenase from the metagenome of the marine sponge *Theonella swinhoei* WA. *ACS Chem. Biol.* 12, 1281–1287. <https://doi.org/10.1021/acscchembio.6b01115>.
- Smitherman, C., Gadda, G., 2013. Evidence for a transient peroxytrio acid in the reaction catalyzed by nitronate monooxygenase with propionate 3-nitronate. *Biochemistry* 52, 2694–2704. <https://doi.org/10.1021/bi400030d>.
- Sobrado, P., Fitzpatrick, P.F., 2003a. Analysis of the role of the active site residue Arg98 in the flavoprotein tryptophan 2-monooxygenase, a member of the L-aminooxidase family. *Biochemistry* 42, 13826–13832. <https://doi.org/10.1021/bi035299n>.
- Sobrado, P., Fitzpatrick, P.F., 2003b. Identification of Tyr413 as an active site residue in the flavoprotein tryptophan 2-monooxygenase and analysis of its contribution to catalysis. *Biochemistry* 42, 13833–13838. <https://doi.org/10.1021/bi035300i>.
- Sole, J., Brummund, J., Caminal, G., Alvaro, G., Schurmann, M., Guillen, M., 2019. Enzymatic synthesis of trimethyl-ε-caprolactone: process intensification and demonstration on a 100 L scale. *Org. Process. Res. Dev.* 23, 2336–2344. <https://doi.org/10.1021/acs.oprd.9b00185>.
- Stewart, J.D., 1998. Cyclohexanone monooxygenase: a useful reagent for asymmetric Baeyer-Villiger reactions. *Curr. Org. Chem.* 195–216.
- Stoisser, T., Brunstner, M., Wilson, D.K., Nidetzky, B., 2016. Conformational flexibility related to enzyme activity: evidence for a dynamic active-site gatekeeper function of Tyr(215) in *Aerococcus viridans* lactate oxidase. *Sci. Rep.* 6, 27892. <https://doi.org/10.1038/srep27892>.
- Sucharitatkul, J., Prongjit, M., Haltrich, D., Chaiyen, P., 2008. Detection of a C4a-hydroperoxyflavin intermediate in the reaction of a flavoprotein oxidase. *Biochemistry* 47, 8485–8490. <https://doi.org/10.1021/bi801039d>.
- Sucharitatkul, J., Tinikul, R., Chaiyen, P., 2014. Mechanisms of reduced flavin transfer in the two-component flavin-dependent monooxygenases. *Arch. Biochem. Biophys.* 555, 33–46. <https://doi.org/10.1016/j.abb.2014.05.009>.
- Sun, W.M., Williams, C.H., Massey, V., 1996. Site-directed mutagenesis of glycine 99 to alanine in L-lactate monooxygenase from *Mycobacterium smegmatis*. *J. Biol. Chem.* 271, 17226–17233.
- Sutton, W.B., 1954. Isolation and properties of a lactic oxidative decarboxylase from *Mycobacterium phlei*. *J. Biol. Chem.* 210, 309–320.
- Sutton, W.B., 1955. Sulfhydryl and prosthetic groups of lactic oxidative decarboxylase from *Mycobacterium phlei*. *J. Biol. Chem.* 216, 749–761.
- Sutton, W.B., 1957. Mechanism of action and crystallization of lactic oxidative decarboxylase from *Mycobacterium phlei*. *J. Biol. Chem.* 226, 395–405.
- Tai, H.H., Bloch, K., 1972. Squalene epoxidase of rat-liver. *J. Biol. Chem.* 247, 3767–3773.
- Tang, M.C., Zou, Y., Watanabe, K., Walsh, C.T., Tang, Y., 2017. Oxidative cyclization in natural product biosynthesis. *Chem. Rev.* 117, 5226–5333. <https://doi.org/10.1021/acs.chemrev.6b00478>.
- Taschner, M.J., Black, D.J., 1988. The enzymatic Baeyer-Villiger oxidation: enantioselective synthesis of lactones from mesomeric cyclohexanones. *J. Am. Chem. Soc.* 110, 6892–6893. <https://doi.org/10.1021/ja00228a053>.
- Taylor, D.G., Trudgill, P.W., 1986. Camphor revisited: studies of 2,5-diketocamphane 1,2-monooxygenase from *Pseudomonas putida* ATCC 17453. *J. Bacteriol.* 165, 489–497. <https://doi.org/10.1128/jb.165.2.489-497.1986>.
- Teufel, R., Miyanaga, A., Michaudel, Q., Stull, F., Louie, G., Noel, J.P., Baran, P.S., Palfey, B., Moore, B.S., 2013. Flavin-mediated dual oxidation controls an enzymatic Favorskii-type rearrangement. *Nature* 503, 552–556. <https://doi.org/10.1038/nature12643>.
- Teufel, R., Stull, F., Meehan, M.J., Michaudel, Q., Dorrestein, P.C., Palfey, B., Moore, B.S., 2015. Biochemical establishment and characterization of EncM's flavin-N5-oxide cofactor. *J. Am. Chem. Soc.* 137, 8078–8085. <https://doi.org/10.1021/jacs.5b03983>.
- Teufel, R., Agarwal, W., Moore, B.S., 2016. Unusual flavoenzyme catalysis in marine bacteria. *Curr. Opin. Chem. Biol.* 31, 31–39. <https://doi.org/10.1016/j.clopa.2016.01.001>.
- Thodberg, S., Neilson, E.J.H., 2020. The “green” FMOs: diversity, functionality and application of plant flavoproteins. *Catalysts* 10, 329. <https://doi.org/10.3390/catal10030329>.
- Thodberg, S., Sorensen, M., Bellucci, M., Crocoll, C., Bendtsen, A.K., Nelson, D.R., Motawia, M.S., Moller, B.L., Neilson, E.H.J., 2020. A flavin-dependent monooxygenase catalyzes the initial step in cyanogenic glycoside synthesis in ferns. *Commun. Biol.* 3, 507. <https://doi.org/10.1038/s42003-020-01224-5>.
- Thoden, J.B., Branch, M.C., Zimmer, A.L., Bruender, N.A., Holden, H.M., 2013. Active site architecture of a sugar N-oxygenase. *Biochemistry* 52, 3191–3193. <https://doi.org/10.1021/bi400407x>.
- Tinikul, R., Chaiyen, P., 2016. Structure, mechanism, and mutation of bacterial luciferase. In: Thouand, G., Marks, R. (Eds.), *Bioluminescence: Fundamentals and Applications in Biotechnology*. Springer International Publishing, Cham, pp. 47–74.
- Tinikul, R., Pitsawong, W., Sucharitatkul, J., Nijvipakul, S., Ballou, D.P., Chaiyen, P., 2013. The transfer of reduced flavin mononucleotide from LuxG oxidoreductase to luciferase occurs via free diffusion. *Biochemistry* 52, 6834–6843. <https://doi.org/10.1021/bi4006545>.
- Tinikul, R., Lawan, N., Akeratchatapan, N., Pimviriyakul, P., Chinantuya, W., Suadee, C., Sucharitatkul, J., Chenprakhon, P., Ballou, D.P., Entsch, B., Chaiyen, P., 2021. Protonation status and control mechanism of flavin-oxygen intermediates in the reaction of bacterial luciferase. *FEBS J.* <https://doi.org/10.1111/febs.15653>. In Press.
- Tischler, D., Eulberg, D., Lakner, S., Kaschabek, S.R., van Berkel, W.J.H., Schlomann, M., 2009. Identification of a novel self-sufficient styrene monooxygenase from *Rhodococcus opacus* 1CP. *J. Bacteriol.* 191, 4996–5009. <https://doi.org/10.1128/Jb.00307-09>.
- Tischler, D., Kermer, R., Groning, J.A.D., Kaschabek, S.R., van Berkel, W.J.H., Schlomann, M., 2010. StyA1 and StyA2B from *Rhodococcus opacus* 1CP: a multifunctional styrene monooxygenase system. *J. Bacteriol.* 192, 5220–5227. <https://doi.org/10.1128/Jb.00723-10>.
- Tischler, D., Schlomann, M., van Berkel, W.J.H., Gassner, G.T., 2013. FAD C(4a)-hydroxide stabilized in a naturally fused styrene monooxygenase. *FEBS Lett.* 587, 3848–3852. <https://doi.org/10.1016/j.febslet.2013.10.013>.
- Tischler, D., Schwabe, R., Siegel, L., Joffroy, K., Kaschabek, S.R., Scholtissek, A., Heine, T., 2018. VpStyA1/VpStyA2B of *Variovorax paradoxus* EPS: an aryl alkyl sulfoxidase rather than a styrene epoxidizing monooxygenase. *Molecules* 23, 809. <https://doi.org/10.3390/molecules23040809>.
- Tischler, D., Kumpf, A., Eggerichs, D., Heine, T., 2020. Styrene monooxygenases, indole monooxygenases and related flavoproteins applied in bioremediation and biocatalysis. In: Chaiyen, P., Tamanoi, F. (Eds.), *The Enzymes*. Academic Press, pp. 399–425.
- Toda, H., Imae, R., Komio, T., Itoh, N., 2012. Expression and characterization of styrene monooxygenases of *Rhodococcus* sp. ST-5 and ST-10 for synthesizing enantiopure (S)-epoxides. *Appl. Microbiol. Biotechnol.* 96, 407–418. <https://doi.org/10.1007/s00253-011-3849-3>.
- Toda, H., Ohuchi, T., Imae, R., Itoh, N., 2015. Microbial production of aliphatic (S)-epoxyalkanes by using *Rhodococcus* sp. strain ST-10 styrene monooxygenase expressed in organic-solvent-tolerant *Kocuria rhizophila* DC2201. *Appl. Environ. Microbiol.* 81, 1919–1925. <https://doi.org/10.1128/Aem.03405-14>.
- Tolmie, C., Smit, M.S., Opperman, D.J., 2019. Native roles of Baeyer-Villiger monooxygenases in the microbial metabolism of natural compounds. *Nat. Prod. Rep.* 36, 326–353. <https://doi.org/10.1039/c8np00054a>.
- Tong, Y., Trajkovic, M., Savino, S., van Berkel, W.J.H., Fraaije, M.W., 2020. Substrate binding tunes the reactivity of hispidin 3-hydroxylase, a flavoprotein monooxygenase involved in fungal bioluminescence. *J. Biol. Chem.* <https://doi.org/10.1074/jbc.RA120.014996>.
- Toplak, M., Matthews, A., Teufel, R., 2021. The devil is in the details: The chemical basis and mechanistic versatility of flavoprotein monooxygenases. *Arch. Biochem. Biophys.* 698, 108732. <https://doi.org/10.1016/j.abb.2020.108732>.
- Torres Pazmino, D.E., Dudek, H.M., Fraaije, M.W., 2010. Baeyer-Villiger monooxygenases: recent advances and future challenges. *Curr. Opin. Chem. Biol.* 14, 138–144. <https://doi.org/10.1016/j.coba.2009.11.017>.
- Trisrivirat, D., Lawan, N., Chenprakhon, P., Matsui, D., Asano, Y., Chaiyen, P., 2020. Mechanistic insights into the dual activities of the single active site of L-lysine oxidase/monooxygenase from *Pseudomonas* sp. AIU 813. *J. Biol. Chem.* 295, 11246–11261. <https://doi.org/10.1074/jbc.RA120.014055>.
- Tsugafune, S., Mashiguchi, K., Fukui, K., Takebayashi, Y., Nishimura, T., Sakai, T., Shimada, Y., Kasahara, H., Koshiba, T., Hayashi, K., 2017. Yucasin DF, a potent and persistent inhibitor of auxin biosynthesis in plants. *Sci. Rep.* 7 <https://doi.org/10.1038/s41598-017-14332-w>.
- Turnaev, I.I., Gunbin, K.V., Suslov, V.V., Akberdin, I.R., Kolchanov, N.A., Afonnikov, D.A., 2020. The phylogeny of class B flavoprotein monooxygenases and the origin of the YUCCA protein family. *Plants-Basel* 9, 1092. <https://doi.org/10.3390/plants9091092>.

- Ukaegbu, U.E., Kantz, A., Beaton, M., Gassner, G.T., Rosenzweig, A.C., 2010. Structure and ligand binding properties of the epoxidase component of styrene monooxygenase. *Biochemistry* 49, 1678–1688. <https://doi.org/10.1021/Bi901693u>.
- Unversucht, S., Hollmann, F., Schmid, A., van Pée, K.-H., 2005. FADH₂-dependence of tryptophan 7-halogenase. *Adv. Synth. Catal.* 347, 1163–1167. <https://doi.org/10.1002/adsc.200505029>.
- Valentino, H., Campbell, A.C., Schuermann, J.P., Sultana, N., Nam, H.G., LeBlanc, S., Tanner, J.J., Sobrado, P., 2020. Structure and function of a flavin-dependent S-monooxygenase from garlic (*Allium sativum*). *J. Biol. Chem.* 295, 11042–11055. <https://doi.org/10.1074/jbc.RA120.014484>.
- van Beek, H.L., de Gonzalo, G., Fraaije, M.W., 2012. Blending Baeyer-Villiger monooxygenases: using a robust BVMO as a scaffold for creating chimeric enzymes with novel catalytic properties. *Chem. Commun.* 48, 3288–3290. <https://doi.org/10.1039/C2cc17656d>.
- van Berkel, W.J.H., Müller, F., 1991. Flavin-dependent monooxygenases with special reference to *p*-hydroxybenzoate hydroxylase. In: Müller, F. (Ed.), *Chemistry and Biochemistry of Flavoenzymes*. CRC Press, pp. 1–30.
- van Berkel, W.J.H., Kamerbeek, N.M., Fraaije, M.W., 2006. Flavoprotein monooxygenases, a diverse class of oxidative biocatalysts. *J. Biotechnol.* 124, 670–689. <https://doi.org/10.1016/j.jbiotec.2006.03.044>.
- van der Bolt, F.J.T., van den Heuvel, R.H.H., Vervoort, J., van Berkel, W.J.H., 1997. ¹⁹F NMR study on the regioselectivity of hydroxylation of tetrafluoro-4-hydroxybenzoate by wild-type and Y385F *p*-hydroxybenzoate hydroxylase: Evidence for a consecutive oxygenolytic dehalogenation mechanism. *Biochemistry* 36, 14192–14201. <https://doi.org/10.1021/bi971213c>.
- van Hellemond, E.W., Janssen, D.B., Fraaije, M.W., 2007. Discovery of a novel styrene monooxygenase originating from the metagenome. *Appl. Environ. Microbiol.* 73, 5832–5839. <https://doi.org/10.1128/Aem.02708-06>.
- van Pée, K.-H., Dong, C.J., Flecks, S., Naismith, J., Patallo, E.P., Wage, T., 2006. Biological halogenation has moved far beyond haloperoxidases. *Adv. Appl. Microbiol.* 59, 127–157. [https://doi.org/10.1016/S0065-2164\(06\)59005-7](https://doi.org/10.1016/S0065-2164(06)59005-7).
- van Thoai, N., Olomucki, A., 1962a. Arginine décarboxy-oxydase. I. Caractères et nature de l'enzyme. *Biochim. Biophys. Acta* 59, 533–544. [https://doi.org/10.1016/0006-3002\(62\)90631-5](https://doi.org/10.1016/0006-3002(62)90631-5).
- van Thoai, N., Olomucki, A., 1962b. Arginine décarboxy-oxydase. II. Oxydation de la canavanine et de l'homoarginine en beta-guanidoxypionamide et en delta-guanidovaleramide. *Biochim. Biophys. Acta* 59, 545–552. [https://doi.org/10.1016/0006-3002\(62\)90632-7](https://doi.org/10.1016/0006-3002(62)90632-7).
- Vervoort, J., Muller, F., Lee, J., van den Berg, W.A.M., Moonen, C.T.W., 1986. Identifications of the true carbon-13 nuclear magnetic resonance spectrum of the stable intermediate II in bacterial luciferase. *Biochemistry* 25, 8062–8067. <https://doi.org/10.1021/bi00372a040>.
- Vey, J.L., Al-Mestarihi, A., Hu, Y.F., Funk, M.A., Bachmann, B.O., Iverson, T.M., 2010. Structure and mechanism of ORF36, an amino sugar oxidizing enzyme in everninomicin biosynthesis. *Biochemistry* 49, 9306–9317. <https://doi.org/10.1021/bi101336u>.
- Waldman, A.J., Ng, T.L., Wang, P., Balskus, E.P., 2017. Heteroatom-heteroatom bond formation in natural product biosynthesis. *Chem. Rev.* 117, 5784–5863. <https://doi.org/10.1021/acs.chemrev.6b00621>.
- Walsh, C.T., Chen, Y.C.J., 1988. Enzymic Baeyer-Villiger oxidations by flavin-dependent monooxygenases. *Angew. Chem. Int. Ed.* 27, 333–343. <https://doi.org/10.1002/anie.198803331>.
- Walsh, C.T., Wencewicz, T.A., 2013. Flavoenzymes: versatile catalysts in biosynthetic pathways. *Nat. Prod. Rep.* 30, 175–200. <https://doi.org/10.1039/c2np20069d>.
- Wang, P., Bashiri, G., Gao, X., Sawaya, M.R., Tang, Y., 2013. Uncovering the enzymes that catalyze the final steps in oxytetracycline biosynthesis. *J. Am. Chem. Soc.* 135, 7138–7141. <https://doi.org/10.1021/ja403516u>.
- Wang, K.K.A., Ng, T.L., Wang, P., Huang, Z.D., Balskus, E.P., van der Donk, W.A., 2018. Glutamic acid is a carrier for hydrazine during the biosyntheses of fosfazinomycin and kinamycin. *Nat. Commun.* 9, 3687. <https://doi.org/10.1038/s41467-018-06083-7>.
- Weijer, W.J., Hofsteenge, J., Vereijken, J.M., Jekel, P.A., Beintema, J.J., 1982. Primary structure of *p*-hydroxybenzoate hydroxylase from *Pseudomonas fluorescens*. *Biochim. Biophys. Acta* 704, 385–388. [https://doi.org/10.1016/0167-4838\(82\)90170-4](https://doi.org/10.1016/0167-4838(82)90170-4).
- Weijer, W.J., Hofsteenge, J., Beintema, J.J., Wierenga, R.K., Drenth, J., 1983. *p*-Hydroxybenzoate hydroxylase from *Pseudomonas fluorescens*. 2. Fitting of the amino acid-sequence to the tertiary structure. *Eur. J. Biochem.* 133, 109–118. <https://doi.org/10.1111/j.1432-1033.1983.tb07435.x>.
- Westphal, A.H., Tischler, D., Heinke, F., Hofmann, S., Gröning, J.A.D., Labudde, D., van Berkel, W.J.H., 2018. Pyridine nucleotide coenzyme specificity of *p*-hydroxybenzoate hydroxylase and related flavoprotein monooxygenases. *Front. Microbiol.* 9, 3050. <https://doi.org/10.3389/fmicb.2018.03050>.
- Wicht, D.K., 2016. The reduced flavin-dependent monooxygenase SfnG converts dimethylsulfone to methanesulfinate. *Arch. Biochem. Biophys.* 604, 159–166. <https://doi.org/10.1016/j.abb.2016.07.001>.
- Wierenga, R.K., Dejong, R.J., Kalk, K.H., Hol, W.G.J., Drenth, J., 1979. Crystal structure of *p*-hydroxybenzoate hydroxylase. *J. Mol. Biol.* 131, 55–73. [https://doi.org/10.1016/0022-2836\(79\)90301-2](https://doi.org/10.1016/0022-2836(79)90301-2).
- Willets, A., 1997. Structural studies and synthetic applications of Baeyer-Villiger monooxygenases. *Trends Biotechnol.* 15, 55–62. [https://doi.org/10.1016/S0167-7799\(97\)84204-7](https://doi.org/10.1016/S0167-7799(97)84204-7).
- Willets, A., 2019. Characterised flavin-dependent two-component monooxygenases from the CAM plasmid of *Pseudomonas putida* ATCC 17453 (NCIMB 10007): ketolactonases by another name. *Microorganisms* 7, 1. <https://doi.org/10.3390/microorganisms7010001>.
- Willets, A., Masters, P., Steadman, C., 2018. Regulation of camphor metabolism: induction and repression of relevant monooxygenases in *Pseudomonas putida* NCIMB 10007. *Microorganisms* 6, 41. <https://doi.org/10.3390/microorganisms6020041>.
- Willrodt, C., Gröning, J.A.D., Nerke, P., Koch, R., Scholtissek, A., Heine, T., Schmid, A., Bühler, B., Tischler, D., 2020. Highly efficient access to (S)-sulfoxides utilizing a promiscuous flavoprotein monooxygenase in a whole-cell biocatalyst format. *ChemCatChem* 12, 4664–4671. <https://doi.org/10.1002/cctc.201901894>.
- Witschel, M., Nagel, S., Egli, T., 1997. Identification and characterization of the two-enzyme system catalyzing oxidation of EDTA in the EDTA-degrading bacterial strain DSM 9103. *J. Bacteriol.* 179, 6937–6943. <https://doi.org/10.1128/jb.179.22.6937-6943.1997>.
- Wu, S., Acevedo, J.P., Reetz, M.T., 2010. Induced allostery in the directed evolution of an enantioselective Baeyer-Villiger monooxygenase. *Proc. Natl. Acad. Sci.* 107, 2775–2780. <https://doi.org/10.1073/pnas.0911656107>.
- Wu, S.K., Liu, J., Li, Z., 2017a. Biocatalytic formal anti-Markovnikov hydroamination and hydration of aryl alkenes. *ACS Catal.* 7, 5225–5233. <https://doi.org/10.1021/acscatal.7b01464>.
- Wu, S.K., Zhou, Y., Seet, D., Li, Z., 2017b. Regio- and stereoselective oxidation of styrene derivatives to arylalkanoic acids via one-pot cascade biotransformations. *Adv. Synth. Catal.* 359, 2132–2141. <https://doi.org/10.1002/adsc.201700416>.
- Xu, Y.R., Mortimer, M.W., Fisher, T.S., Kahn, M.L., Brockman, F.J., Xun, L.Y., 1997. Cloning, sequencing, and analysis of a gene cluster from *Chelatobacter heintzii* ATCC 29600 encoding nitrilotriacetate monooxygenase and NADH:flavin mononucleotide oxidoreductase. *J. Bacteriol.* 179, 1112–1116. <https://doi.org/10.1128/jb.179.4.1112-1116.1997>.
- Xu, N., Zhu, J., Wu, Y.Q., Zhang, Y., Xia, J.Y., Zhao, Q., Lin, G.Q., Yu, H.L., Xu, J.H., 2020. Enzymatic preparation of the chiral (S)-sulfoxide drug esomeprazole at pilot-scale levels. *Org. Process. Res. Dev.* 24, 1124–1130. <https://doi.org/10.1021/acs.oprd.0c00115>.
- Xun, L.Y., Reeder, R.B., Plymale, A.E., Girvin, D.C., Bolton, H., 1996. Degradation of metal-nitrilotriacetate complexes by nitrilotriacetate monooxygenase. *Environ. Sci. Technol.* 30, 1752–1755. <https://doi.org/10.1021/es9507628>.
- Yamamoto, S., Katagiri, M., Maeno, H., Hayaishi, O., 1965. Salicylate hydroxylase, a monooxygenase requiring flavin adenine dinucleotide. *J. Biol. Chem.* 240, 3408–3413.
- Yamanaka, K., Ryan, K.S., Gulder, T.A.M., Hughes, C.C., Moore, B.S., 2012. Flavoenzyme-catalyzed atropo-selective *N,C*-bipyrrrole homocoupling in marinopyrrole biosynthesis. *J. Am. Chem. Soc.* 134, 12434–12437. <https://doi.org/10.1021/ja305670f>.
- Yeh, E., Garneau, S., Walsh, C.T., 2005. Robust in vitro activity of RebF and RebH, a two-component reductase/halogenase, generating 7-chlorotryptophan during rebeccamycin biosynthesis. *Proc. Natl. Acad. Sci.* 102, 3960–3965. <https://doi.org/10.1073/pnas.0500755102>.
- Yu, H., Zhao, S.X., Lu, W.D., Wang, W., Guo, L.Z., 2018. A novel gene, encoding 3-aminobenzoate 6-monooxygenase, involved in 3-aminobenzoate degradation in *Comamonas* sp. strain QT12. *Appl. Microbiol. Biotechnol.* 102, 4843–4852. <https://doi.org/10.1007/s00253-018-9015-4>.
- Zabala, A.O., Xu, W., Chooi, Y.H., Tang, Y., 2012. Characterization of a silent azaphilone gene cluster from *Aspergillus niger* ATCC 1015 reveals a hydroxylation-mediated pyran-ring formation. *Chem. Biol.* 19, 1049–1059. <https://doi.org/10.1016/j.chembiol.2012.07.004>.
- Zhang, Y., Liu, F., Xu, N., Wu, Y.Q., Zheng, Y.C., Zhao, Q., Lin, G.Q., Yu, H.L., Xu, J.H., 2018. Discovery of two native Baeyer-Villiger monooxygenases for asymmetric synthesis of bulky chiral sulfoxides. *Appl. Environ. Microbiol.* 84. <https://doi.org/10.1128/AEM.00638-18.e00638-00618>.
- Zhang, Y., Wu, Y.Q., Xu, N., Zhao, Q., Yu, H.L., Xu, J.H., 2019. Engineering of cyclohexanone monooxygenase for the enantioselective synthesis of (S)-omeprazole. *ACS Sustain. Chem. Eng.* 7, 7218–7226. <https://doi.org/10.1021/acssuschemeng.9b00224>.
- Zhao, Y.D., Christensen, S.K., Fankhauser, C., Cashman, J.R., Cohen, J.D., Weigel, D., Chory, J., 2001. A role for flavin monooxygenase-like enzymes in auxin biosynthesis. *Science* 291, 306–309. <https://doi.org/10.1126/science.291.5502.306>.
- Zhu, X.F., De Laurentis, W., Leang, K., Herrmann, J., Lhiefeld, K., van Pée, K.-H., Naismith, J.H., 2009. Structural insights into regioselectivity in the enzymatic chlorination of tryptophan. *J. Mol. Biol.* 391, 74–85. <https://doi.org/10.1016/j.jmb.2009.06.008>.
- Zhu, Y., Li, H.J., Su, Q., Wen, J., Wang, Y.F., Song, W., Xie, Y.P., He, W.R., Yang, Z., Jiang, K., Guo, H.W., 2019. A phenotype-directed chemical screen identifies ponalrestat as an inhibitor of the plant flavin monooxygenase YUCCA in auxin biosynthesis. *J. Biol. Chem.* 294, 19923–19933. <https://doi.org/10.1074/jbc.RA119.010480>.
- Ziegler, D.M., 1988. Flavin-containing monooxygenases: catalytic mechanism and substrate specificities. *Drug Metab. Rev.* 19, 1–32. <https://doi.org/10.3109/03602538809049617>.
- Ziegler, D.M., 2002. An overview of the mechanism, substrate specificities, and structure of FMOs. *Drug Metab. Rev.* 34, 503–511. <https://doi.org/10.1081/Dmr-120005650>.
- Ziegler, D.M., Mitchell, C.H., 1972. Microsomal oxidase IV: properties of a mixed-function amine oxidase isolated from pig liver-microsomes. *Arch. Biochem. Biophys.* 150, 116–125. [https://doi.org/10.1016/0003-9861\(72\)90017-3](https://doi.org/10.1016/0003-9861(72)90017-3).